



**NIST Internal Report
NIST IR 8451**

Multi'omic Characterization of Human Whole Stool RGTMs

Amanda Bayless
Sandra Da Silva
W. Clay Davis
Abraham Kuri Cruz
Paulina Piotrowski
Tracey Schock
Stephanie Servetas

This publication is available free of charge from:
<https://doi.org/10.6028/NIST.IR.8451>

**NIST Internal Report
NIST IR 8451**

**Multi'omic Characterization of
Human Whole Stool RGTMs**

Amanda Bayless
W. Clay Davis
Abraham Kuri Cruz
Paulina Piotrowski
Tracey Schock
*Chemical Sciences Division
Material Measurement Laboratory*

Sandra Da Silva
Stephanie Servetas
*Biosystems and Biomaterials Division
Material Measurement Laboratory*

This publication is available free of charge from:
<https://doi.org/10.6028/NIST.IR.8451>

September 2023



U.S. Department of Commerce
Gina M. Raimondo, Secretary

National Institute of Standards and Technology
Laurie E. Locascio, NIST Director and Under Secretary of Commerce for Standards and Technology

NIST IR 8451
September 2023

NIST Disclaimer

All opinions expressed in this report are the authors' and do not necessarily reflect the policies and views of NIST or affiliated venues. Certain pieces of commercial equipment, instruments, or materials are identified in this paper to specify the experimental procedure adequately. Such identification is not intended to imply recommendation or endorsement by the National Institute of Standards and Technology, nor is it intended to imply that the materials or equipment identified are necessarily the best available for the purpose.

NIST Technical Series Policies

[Copyright, Use, and Licensing Statements](#)

[NIST Technical Series Publication Identifier Syntax](#)

Publication History

Approved by the NIST Editorial Review Board on 2023-08-09

How to Cite this NIST Technical Series Publication

Bayless A, Da Silva S, Davis WC, Cruz AK, Piotrowski P, Schock T, Servetas S (2023), Multi'omic Characterization of Human Whole Stool RGTMs. (National Institute of Standards and Technology, Gaithersburg, MD), NIST Internal Report (IR) NIST IR 8451. <https://doi.org/10.6028/NIST.IR.8451>

NIST Author ORCID iDs

Amanda Bayless: 0000-0002-9073-5582

Sandra Da Silva: 0000-0002-7121-7544

W. Clay Davis: 0000-0001-9076-2620

Abraham Kuri Cruz: 0000-0003-4409-0653

Paulina Piotrowski: 0000-0002-8039-7911

Tracey Schock: 0000-0002-1808-7816

Stephanie Servetas: 0000-0002-4924-4511

Contact Information

sandra.dasilva@nist.gov

stephanie.servetas@nist.gov

Abstract

The gut microbiome plays a critical role in a vast and disparate set of health and disease states, including cancer and obesity. Human fecal is a complex mixture including microbes, proteins, undigested plant matter and fat content according to the diet type (e.g., vegan, omnivore). The complexity of human fecal material along with the complexity of the analytical workflow of omics-based techniques makes measurements such as metabolomics and metagenomics challenging. To address this need, NIST is developing a human stool reference material (RM) to compare and assess reproducibility in omics-based techniques. This report shares the initial characterization of a human stool research grade testing material (RGTM). At NIST, a RGTM is an exploratory material developed to evaluate the feasibility of a given designed material. The set of RGTMs is a precursor of the actual RM and is composed of (RGTMs 10162 (Vegan-Lyophilized), 10171 (Vegan-Aqueous), 10172 (Omnivore-lyophilized), 10173 (Omnivore-Aqueous)). The RGTMs were characterized by LC-MS, GC-MS, ¹H NMR and whole genome sequencing (WGS). The effort to develop a human whole stool reference material started in 2019 and since then, protocols to analyze the samples have been optimized. The approaches used to characterize the samples described in this report may or may not be the current approach used on the characterization of the reference material, RM8048. In addition, it should be stated the material used in the RGTM and consequently in the RM is not an authentic representation of human stool as it was processed (homogenized, diluted in water and bottled) after collection for research application.

Keywords

Human whole stool; Gas chromatography; Liquid chromatography; Nuclear magnetic resonance; Mass spectrometry; Metabolomics; Metagenomics; Research grade testing material

Table of Contents

1. Introduction	1
2. Material Production	1
3. Metagenomic Characterization	2
3.1. Methods.....	2
3.2. Results and Discussion.....	2
4. Stool Characterization via LC-MS	13
4.1 . Methods.....	13
4.2. Results and Discussion.....	16
5. Stool Characterization via GC-MS	24
5.1. Methods.....	24
5.2. Results and Discussion.....	24
6. Stool Characterization via ¹H NMR	27
6.1. Methods.....	27
6.2. Results and Discussion.....	28
7. Conclusion	33
8. References	35
Appendix A. Genera and Relative Abundance for 10 replicate Vegan aliquots.	36
Taxonomy ID	36
Appendix B. Genera and Relative Abundance for 10 replicate Omnivore aliquots	39
Appendix C. Metabolite concentration (mM) in the NMR sample extract relative to the TMSP chemical shift reference standard. Four vials were analyzed per each sample.	42
Appendix D. Glossary	44

List of Tables

Table 1. Relative Abundance and CV values for Phyla detected in Vegan and Omnivore Aliquots.	6
Table 2. Top 20 most abundant metabolites by LC-HRMS for each sample type as identified by MS/MS spectral library. (Polar extract – positive mode). Metabolites observed in the same order across all samples (green), metabolites observed across all samples, but order is inconsistent (yellow), metabolites observed across some samples (blue) and metabolites only observed in one sample (pinkish-orange).	18
Table 3. Top 20 most abundant metabolites by LC-HRMS for each sample type as identified by MS/MS spectral library matching (Polar extract – negative mode). Metabolites observed in the same order across all samples (green), metabolites observed across all samples, but order is inconsistent (yellow), metabolites observed across some samples (blue) and metabolites only observed in one sample (pinkish-orange).	19
Table 4. Top 20 most abundant metabolites by LC-HRMS for each sample type as identified by MS/MS spectral library matching (Non-polar extract – positive mode). Metabolites observed in the same order across all samples (green), metabolites observed across all samples, but order is inconsistent (yellow), metabolites observed across some samples (blue) and metabolites only observed in one sample (pinkish-orange).	21
Table 5. Top 20 most abundant metabolites by LC-HRMS for each sample type as identified by MS/MS spectral library matching (Non-polar extract – negative mode). Metabolites observed in the same order across all samples (green), metabolites observed across all samples, but order is inconsistent (yellow), metabolites observed across some samples (blue) and metabolites only observed in one sample (pinkish-orange).	22
Table 6. Top 20 metabolites based on relative abundance detected and identified by GCxGC-TOFMS. The table describes metabolites observed in the same order across all samples (green), metabolites observed across all samples, but order is inconsistent (yellow), metabolites observed across some samples (blue) and metabolites only observed in one sample (pinkish-orange).	26
Table 7. Top 20 metabolites per stool material obtained via 1H NMR. The table describes metabolites observed in the same order across all samples (green), metabolites observed across all samples, but order is inconsistent (yellow), metabolites observed across some samples (blue) and metabolites only observed in one sample (pinkish-orange).	32

List of Figures

Figure 1. Human stool homogenization and aliquoting process.	2
Figure 2. Genus level taxonomic profile from vegan and omnivore samples. Barchart shows relative abundance for genera in vegan (blue) fecal samples. A total of 20 aliquots were analyzed, 5 replicates of 4 different samples: Vegan-lyophilized (1-5), Vegan-aqueous (6-10), Omnivore-lyophilized (11-15), Omnivore-aqueous (16-20). For readability, the lowest abundance samples totaling 5% of each sample are grouped as ‘other’.....	4
Figure 3. Diversity metrics. (a) Number of genera present in each cohort. (b) Shannon diversity (c) Inverse Simpson Diversity are also shown for each cohort. Color and shape indicate the type of preservation that was used for the sample. Pink triangles represent aqueous samples (Aq), suspended in water and stored at -80 °C; Dark blue diamonds represent lyophilize samples (Lyo). The green X denotes the mean value for all samples from a given cohort.	4
Figure 4. Comparison of the relative abundances for the Phyla present in vegan and omnivore aliquots. Bacteria_u_p indicate sequences that matched to the bacterial kingdom but not a specific Phyla. Vegan-lyophilized (1-5), Vegan-aqueous (6-10), Omnivore-lyophilized (11-15), Omnivore-aqueous (16-20).....	5
Figure 5. PCoA showing Bray-Curtis dissimilarity index. Omnivore samples are in red, vegan samples shown in turquoise. As in Figure 3, triangles indicate aqueous samples (Aq) and diamond indicate lyophilized (Lyo).	6
Figure 6. Principal component analysis scores plot (PC1 vs. PC2) of polar sample extracts from omnivore aqueous (OA), omnivore lyophilized (OL), vegan aqueous (VA), and vegan lyophilized (VL). The ellipses indicate the 95% confidence interval.	16
Figure 7. Principal component analysis scores plot (PC1 vs PC2) of non-polar sample extracts from omnivore aqueous (OA), omnivore lyophilized (OL), vegan aqueous (VA), and vegan lyophilized (VL). The ellipses indicate the 95% confidence interval.	17
Figure 8. The GCxGC-TOFMS total ion chromatograms for omnivore aqueous, omnivore lyophilized, vegan aqueous, and vegan lyophilized samples.	25
Figure 9. NMR spectra of human stool samples.....	29
Figure 10. Relative concentrations of the 45 compounds identified from ¹ H NMR spectra across the stool materials. Four vials were analyzed (n = 4) for each stool material.	30
Figure 11. Physical characteristic of the stool samples extracted in water after centrifugation for removal of debris.....	31

Acknowledgments

Institute for the Advancement of Food and Nutrition (IAFNS, formerly ILSI North America) provided financial support for the development of the RGTMs.

Christina Jones and Katrice Lippa provided their expertise and support in envisioning this effort.

1. Introduction

The National Institute of Standards and Technology (NIST) has undertaken the endeavor to develop a Human Gut Microbiome (Whole Stool) Reference Material for measurement harmonization and quality assurance/quality control for stool-based metagenomics, metabolomics, and clinical measurements. The most common measurements used in microbiome research and sample testing laboratories are next generation sequencing (NGS) based metagenomics, mass spectrometry-based metabolomics and ^1H NMR based metabolomics. Despite efforts, no fit-for-purpose standards exist that enable researchers to compare results generated across different laboratories and to assess the impact of the multitude of methodological variables that exist in either measurement platform or associated preparative workflow [1-4]. To begin to understand the biologically relevant properties of the human gut microbiome [5-7], the community needs such standards for confident identification of new biomarkers and bacterial strains and/or communities that may serve as disease indicators while supporting the validation of analytical measurements for clinically relevant metabolites and bacterial composition. To address some of these needs, four candidate human whole stool reference materials, RGTMs 10162- vegan lyophilized, 10171- vegan aqueous, 10172- omnivore lyophilized, and 10173- omnivore aqueous were developed in collaboration with The Biocollective (TBC) and ILSI North America. The purpose of this report is to document the initial analysis of the RGTMs with metagenomics, and NMR, LC-MS, and GC-MS metabolomics to assess the sample homogeneity as well as metabolomic and metagenomic profiles of the material.

2. Material Production

Collection and Sample Preparation. Human whole stool was obtained from multiple volunteer donors by TBC (Denver, CO, USA). All whole stool samples were collected after informed consent under approved IRB protocols at TBC. This material is transferred to NIST under an MTA, and the NIST protocols have been deemed non-human subject research by the NIST Research Protection Office. Stool samples were collected from eight (8) volunteer donors: 2 vegan females, 2 vegan males, 2 omnivore females, and 2 omnivore males. Volunteers were matched by age, sex, and body mass index (BMI) and were all surveyed for health and diet. Samples were deposited into a BioCollectorTM and shipped overnight on an ice brick (sample temperature was maintained at approx. 4 °C). Upon receipt, each sample was segmented into 30 g to 50 g portions, stored in specimen collection jars, and placed at -80 °C until processing. A portion of the first stool sample from each donor was subjected to pathogen screening for HIV, Hepatitis B, and Hepatitis C using the Biogates One Step Rapid Diagnostic Tests. The material was prepared by TBC and an overview of the production process is shown in **Figure 1**. All aliquots (lyophilized and aqueous) were shipped to NIST on dry ice and placed immediately into -80 °C storage upon arrival.

During the manufacturing of the RGTMs, NIST had the opportunity to participate in the production workflow, which gave us valuable insight into production process for a homogenized fecal material. Observing the manufacturing process and recoding the details allowed us to identify points where measurement variability could be introduced; this is very helpful for planning future productions. We also observed that during the process of material homogenization in water, a white-to-cream colored ring adhered at the air-liquid interface of the glass flask, which suggests being hydrophobic compounds.

This was more pronounced in the omnivore samples. Most of this white-to-cream layer was left behind in the container and not aliquoted implying that the final material might not contain its full lipid components. In future productions, care will be taken to create a naturally representative material that encompasses the full breadth of typical components.

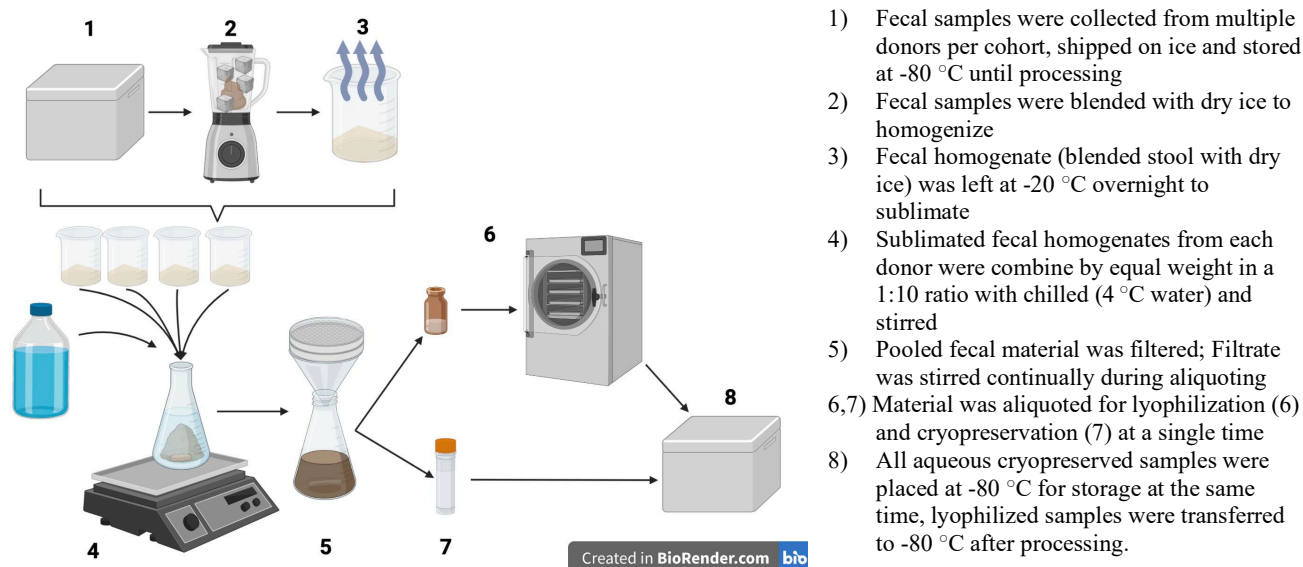


Figure 1. Human stool homogenization and aliquoting process.

3. Metagenomic Characterization

3.1. Methods

DNA extraction and sequencing. Metagenomics data collection for the RGTMs was conducted by CosmosID (Rockville, MD, USA). Twenty samples (5 samples per each RGTM 10162, 10171, 10172, and 10173) were sent to CosmosID. All samples packaged on dry ice and hand delivered to CosmosID where they were stored at -80 °C until processing. DNA extraction (Qiagen Powersoil), library preparation (Illumina Nextera XT), whole genome sequencing (Illumina HiSeq X), and bioinformatics analysis (2020-07-20 v1.0.2) was all completed by CosmosID and the final results were provided in the CosmosID application (<https://app.cosmosid.com/>). Alpha and beta diversity analyses were done in R (version 4.1.0) using vegan v2.6-4.

3.2. Results and Discussion

Taxonomic Classification and Data Analysis. CosmosID generated an average of 6×10^6 reads per sample (range of 4×10^6 reads to 9×10^6 reads per sample). There were no significant differences in number of reads based on diet or preservation method, which is likely since samples are normalized during library preparation to achieve similar read depth. Bacterial taxonomic classification was carried out using whole genome shotgun sequencing and CosmosID's algorithms and bacterial database with the filtered dataset. Across all samples $\leq 1.5\%$ of reads were classified as bacteria with an unknown phylum based on the CosmosID database (v1.0.2).

The objectives for this preliminary metagenomic data analysis were to: (1) provide an initial characterization of the community composition, (2) assess homogeneity of each cohort, and (3) evaluate if there was an effect of preservation method. It is important to note that taxonomic data analysis can be done for multiple taxonomic levels. For the purposes of the study, we will be describing the taxonomic identity and relative abundance at the Genus and Phyla level. For future characterizations, the same types of analyses can be done at any of the taxonomic levels.

Characterization of Community Composition. A total of 89 genera were identified: 77 Genera in the omnivore aliquots and 79 genera in the vegan aliquots (**Appendices A & B**). This data is summarized in **Figure 2** and **Figure 3a**. Fifty-one genera were present in all 10 omnivore aliquots accounting for at least 99% of the composition of each aliquot; the remaining 26 species were not present in all aliquots. The number of genera present in omnivore aliquots ranged from 58-71. Ten genera were identified only in the omnivore sample and 40% (4/10) were present in all omnivore aliquots. These 4 genera (*Abisella*, *Dielma*, *Poryphyromonas*, and *Propionibacterium*) account for less than approximately 0.5% of each aliquot. Forty-nine genera were common to all vegan aliquots, accounting for at least 99% of the composition of each aliquot and 30 genera were found to be variably present. The total number of genera found in each vegan aliquot ranged from 50-70. Twelve genera were found only in the vegan samples, of these 42% (5/12) were present in all aliquots. These 5 genera (*Catenibacterium*, *Desulfovibrio*, *Leuconostoc*, *Methanobrevibacter*, *Senegalimassilia*) account for 2-3% of each aliquot.

We also assessed the alpha diversity, a measurement of community diversity, of each cohort using two metrics: Shannon diversity and Inverse Simpson (**Figure 3b, c**). We chose to visual these metrics for each cohort and preservation method. Both Shannon and Inverse Simpson metrics take the evenness (relative abundance) and richness (number of species) of a community into account. The Shannon diversity index values range from 0-5, with 0 indicative of a single taxa. The minimum value for the Inverse Simpson index is 1, indicating a single taxa and the maximum value is achieved when all taxa are present at the same abundance (perfect evenness) in which case the value is the number of taxa present.

For the analyses shown in **Figure 3** we did not subsample to an equal number of reads; however, we did look for a correlation between read number and higher diversity scores or genera identified. In some cases, for example the sample with the highest number of omnivore genera (71) identified, there was a correlation with the highest number of reads (9.1×10^6). In contrast, the omnivore sample with the second highest number of reads (7.5×10^6) had the lowest number of genera for this cohort (58). For future studies we will look at both full and rarefied datasets.

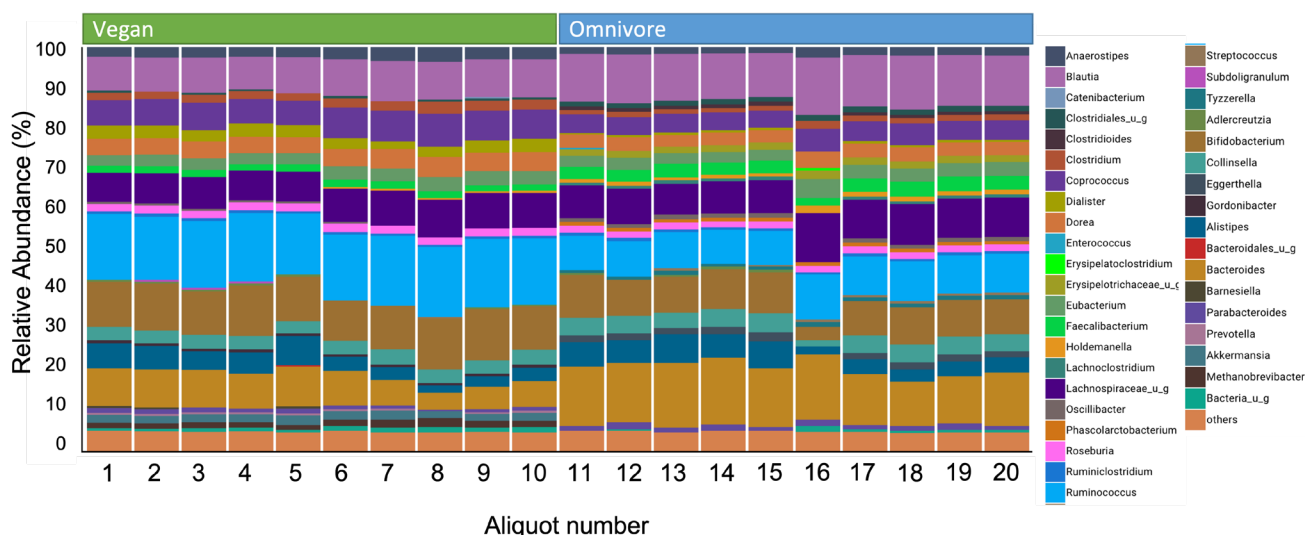


Figure 2. Genus level taxonomic profile from vegan and omnivore samples. Barchart shows relative abundance for genera in vegan (blue) fecal samples. A total of 20 aliquots were analyzed, 5 replicates of 4 different samples: Vegan-lyophilized (1-5), Vegan-aqueous (6-10), Omnivore-lyophilized (11-15), Omnivore-aqueous (16-20). For readability, the lowest abundance samples totaling 5% of each sample are grouped as ‘other’.

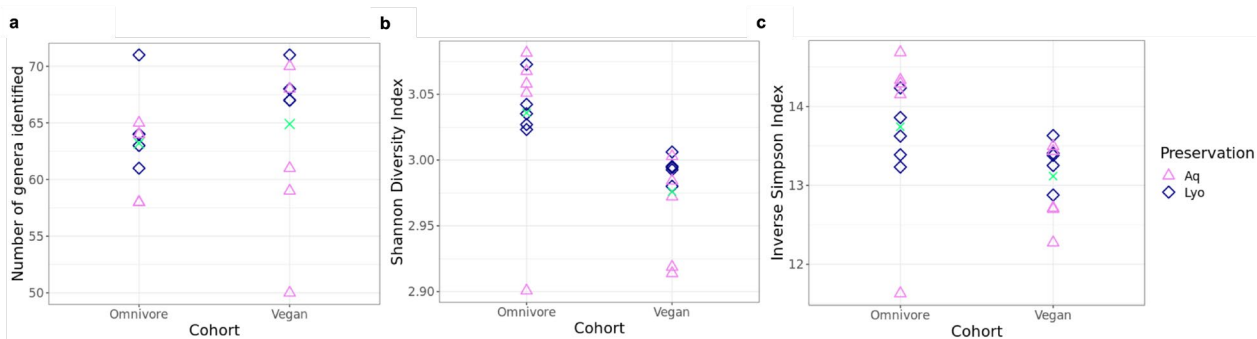


Figure 3. Diversity metrics. (a) Number of genera present in each cohort. (b) Shannon diversity (c) Inverse Simpson Diversity are also shown for each cohort. Color and shape indicate the type of preservation that was used for the sample. Pink triangles represent aqueous samples (Aq), suspended in water and stored at -80°C ; Dark blue diamonds represent lyophilize samples (Lyo). The green X denotes the mean value for all samples from a given cohort.

Homogeneity Assessment. Based presence of genera identified by a single workflow, both cohorts appear to be homogenous with respect to the most abundant genera (99% of the composition). Heterogeneity is observed for genera that are present at relative abundances of $< 0.3\%$ and $< 0.5\%$ in the omnivore and vegan cohorts, respectively. With the current samples we are unable to determine if the heterogeneity is due to the measurement pipeline, if rare genera have heterogenous distribution across the aliquots, or if it is a combination.

Another way to assess homogeneity is to compare the relative abundance values between samples on a taxa-by-taxa basis. This analysis could be conducted at any taxonomic level and for simplicity in this pilot study we evaluated the samples at the Phylum level (Figure 4). The relative abundance values for one of the aqueous omnivore aliquots, sample 16, appeared distinct from the other omnivore samples.

In fact, Actinobacteria, Synergistetes, Verrucomicrobia, and reads classified as Bacteria with an unassigned phylum (Bacteria_u_p) were all identified as outliers compared with the other aliquots (GraphPad Prism v 9.1.0 ROUT analysis, Q= 1%). Additionally, sample 16 appears distinct from the other omnivore samples recording the lowest alpha-diversity score for both Shannon and Inverse Simpson (**Figure 3b, c**). Replicate measurements and aliquots should be examined to determine if these differences were due to an experimental error or an indication of greater variability in aliquots. We further examined the variability of the relative abundance values by calculating the coefficient of variation (CV) for each Phyla from a given cohort; sample 16 was excluded from this analysis. The CV for the vegan aliquots ranged from 5.6 % - 88.7 % and for the omnivore aliquots from 6.5 % - 28.8 % (**Table 1**). The Phyla with the highest CVs were Synergistetes (88.68 %) and Bacteria_u_p (28.8 %) for the vegan and omnivore cohorts, respectively. Both were present at a relative abundance of <1 %. It is unclear what an acceptable CV for a given taxa will be and this will be a point of discussion for the final reference material.

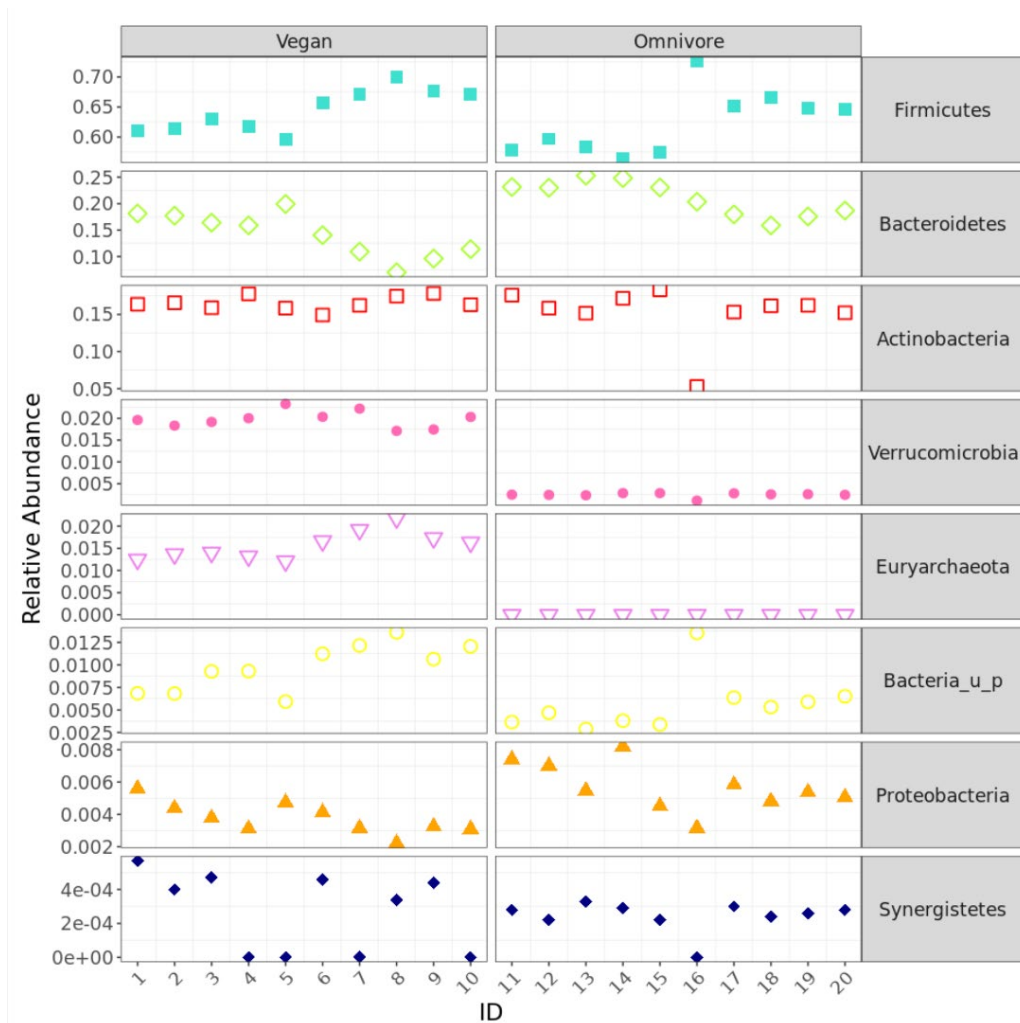


Figure 4. Comparison of the relative abundances for the Phyla present in vegan and omnivore aliquots. Bacteria_u_p indicate sequences that matched to the bacterial kingdom but not a specific Phyla. Vegan-lyophilized (1-5), Vegan-aqueous (6-10), Omnivore-lyophilized (11-15), Omnivore-aqueous (16-20).

Table 1. Relative Abundance and CV values for Phyla detected in Vegan and Omnivore Aliquots.

Phylum	Vegan				Omnivore			
	Mean	CV-all	CV-Lyo	CV-Aq	Mean	CV-all	CV-Lyo	CV-Aq
Firmicutes	0.6445	5.46%	2.01%	2.29%	0.6239	6.50%	5.00%	1.40%
Bacteroidetes	0.1411	29.85%	9.01%	24.24%	0.2098	16.65%	9.01%	6.78%
Actinobacteria	0.1652	5.60%	4.72%	6.94%	0.1523	6.88%	34.38%	3.40%
Verrucomicrobia	0.0198	9.83%	9.45%	11.10%	0.0024	7.08%	29.22%	5.45%
Euryarchaeota	0.0157	20.15%	6.21%	12.44%				
Bacteria_u_p	0.0098	26.61%	20.39%	9.44%	0.0056	28.78%	45.10%	8.97%
Proteobacteria	0.0037	26.25%	21.84%	21.30%	0.0057	21.42%	20.96%	8.31%
Synergistetes	0.0003	88.68%	93.67%	93.11%	0.0002	13.85%	56.85%	9.56%

Effect of Preservation Method. As noted above, we chose to visual the diversity metrics for each cohorts based on preservation method (Figure 3). While there may appear to be higher variability for the alpha diversity metrics (pink vs blue), especially in the vegan samples, these differences were not significant (Two-tailed T-Test) (Figure 3). Furthermore, looking at the principle coordinate analysis (PCoA) of the Bray-Curtis dissimilarity index that assess the relatedness of two samples based on composition, we can see that any effect of the preservation method is minor compared to the difference in cohorts (vegan and omnivore) (Figure 5). Notably, the same omnivore aqueous sample where we observed outliers when comparing relative abundance values (Sample 16) showed up distinct from the rest of the cluster in this analysis. When this sample is removed the PCoA replotted, some clustering by preservation method (diamonds vs triangles) is observed; however, the y-axis scale (separating preservation) is very small relative to the x-axis (separating cohort) (Figure 5b). Finally, given the some of the high CVs observed in the Phyla relative abundance analysis (Figure 4) we also assessed whether separating samples by preservation method would result in smaller CVs (Table 1). For most taxa there was a reduction in CV, but for others the CV either increased or stayed the same. Overall, the preservation method of choice did not dramatically impact the results and either would be fit for purpose.

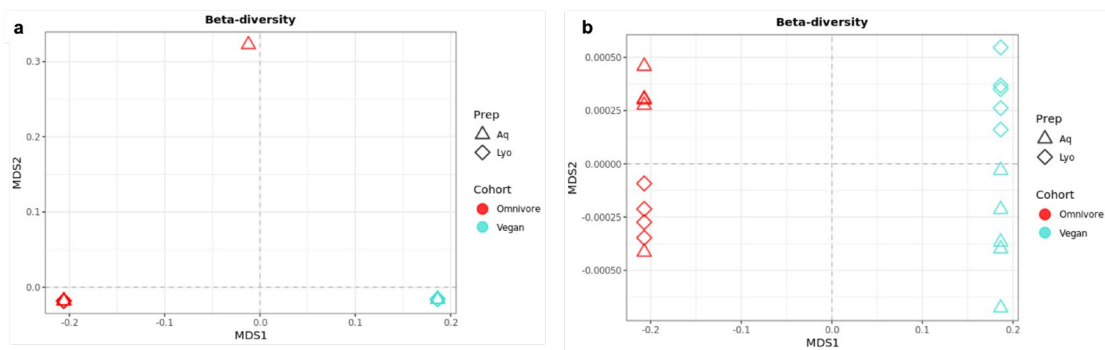


Figure 5. PCoA showing Bray-Curtis dissimilarity index. Omnivore samples are in red, vegan samples shown in turquoise. As in Figure 3, triangles indicate aqueous samples (Aq) and diamond indicate lyophilized (Lyo).

4. Stool Characterization via LC-MS

4.1. Methods

Sample Extraction for Mass Spectrometry Metabolomics. To comprehensively capture the metabolites from the aqueous storage solution, a liquid-liquid extraction (subsection ‘Aqueous Supernatant Extraction’) was combined with the stool particulate extracts (subsection ‘Stool Particulate Extraction’).

Aqueous Supernatant Extraction. Lyophilized stool samples (n=3/diet) were re-hydrated with 1 mL of cold deionized (DI) water and gently inverted to mix sample. Rehydrated samples were then transferred to a clean 2 mL cryovial and placed on ice. Due to large particles, transfer was completed by cutting a 200 μ L pipette tip to 1st marked line with solvent-cleaned scissors. Fresh-frozen aqueous stool samples (n=3/diet) were removed from -80 °C freezer and placed on ice to thaw for 20 min. Upon thawing, wet sample was transferred to a clean, labeled 2 mL cryovial (Thermo Scientific Nalgene, USA) and placed on ice. All samples were then pelleted via centrifugation in a centrifuge at 4000 rpm for 10 min at 4 °C. The aqueous supernatant was then transferred to a 10 mL glass tube (Corning) containing cold chloroform (CHCl_3). The cryovials with the pelleted samples were placed on ice while working with aqueous supernatant. The glass tubes with the aqueous supernatant in CHCl_3 were then vortexed for 30 s and phases were allowed to separate on ice for 5 min. The aqueous phase was then transferred to a clean, labeled, tared microcentrifuge tube, and concentrated in Vacufuge concentrator while the non-polar CHCl_3 phase was transferred to glass vials and concentrated in a Turbovap under a gentle stream of N_2 gas.

Internal Standard Preparation. QReSS IS kit (Cambridge isotope lot # PR-31438) was prepared per manufacturers recommendations by adding 1 mL of 50 % (v/v) MeOH in H_2O to each vial and stored at -80 °C. Prior to LC-MS sample preparation, 0.45 mL from each vial was diluted to 1.1 mL in 50 % (v/v) MeOH in H_2O .

Stool Particulate Extraction. The individual pelleted stool masses, along with four aliquots (50 mg \pm 0.05 mg) of SRM 2781 Domestic Sludge for quality control, were then extracted by a modified Bligh-Dyer method by adding 0.51 mL of cold polar solvent (60 % (v/v) MeOH in water and 0.05 mL of QReSS IS to each tube and vortexing the samples for 60 s. The sample slurry mixture was then transferred to glass tubes containing the nonpolar solvent (2:1 volume ratio of $\text{CHCl}_3/\text{H}_2\text{O}$), vortex mixed for 60 s, and placed on ice for 10 min. To ensure phase separation, the glass tubes were spun in a centrifuge at 4000 rpm for 10 min at 4 °C. The polar fraction of the Bligh-Dyer (upper phase) was combined with the dried aqueous extract (from the section above) and concentrated in Vacufuge concentrator while the non-polar (lower-phase) was combined with the dried non-polar extract (from the section above) and concentrated in a Turbovap under a gentle stream of N_2 gas. The masses of all recovered extracts were recorded. Prior to LC-MS analysis, samples were re-constituted in 2% (v/v) MeOH in water (polar extract) or in 60:40 (v/v) acetonitrile:water (non-polar extract) and transferred to autosampler vials.

LC/-MS Analysis (Polar Extract). Samples were analyzed using a Vanquish UPLC coupled to a Fusion Lumos mass spectrometer (Thermo Fisher Scientific). Reconstituted samples (1 μL injection volume) were separated by an Acquity HSS T3 (1.8 μm , 2.1 mm id x 150 mm length; Waters) C18 column at 350 $\mu\text{L}/\text{min}$ and 45 $^{\circ}\text{C}$ with the gradient program listed in Table 2. The mass spectrometer was operated in positive polarity, default source parameters for the flow rate, and data dependent mode (topN, 1 s cycle time) with a dynamic exclusion of 10 s (with 10 ppm error). The RF lens was set at 60 %. Full scan resolution using the orbitrap was set at 120,000 and the mass range was set to m/z 100 amu to 1000 amu. Full scan ion target value was 5.0×10^5 allowing a maximum injection time of 50 ms. Monoisotopic peak determination was used, specifying small molecule, and an intensity threshold of 2.5×10^4 was used for precursor selection. Data-dependent fragmentation was performed using higher-energy collisional dissociation (HCD) with a stepped collision energy of 20, 30, and 50 with quadrupole isolation at m/z 1.5 width. The fragment scan resolution using the orbitrap was set at 15,000, ion target value of 5.0×10^4 and 22 ms maximum injection time. An additional analysis utilizing the same separation method and mass spectrometer settings in negative mode was also performed.

An additional analytical run for each stool sample group was performed in Acquire X data acquisition mode to provide additional MS2 data used for spectral library matching and annotation. The MS1 method for determining the initial exclusion list from the blank and inclusion list from the sample was run with an orbitrap resolution of 120,000, mass range of m/z 67 amu to 1000 amu, and an ion target value of 1.0×10^5 allowing a maximum injection time of 50 ms. For the subsequent data-dependent acquisition (DDA) acquisition runs, the mass spectrometer was operated in positive polarity, default source parameters for the flow rate, and data dependent mode (topN, 1 s cycle time) with a dynamic exclusion of 2.5 s (with 10 ppm error). The RF lens was set at 60 %. Full scan resolution using the orbitrap was set at 120,000 and the mass range was set to m/z 67 amu to 1000 amu. Full scan ion target value was 1.0×10^5 allowing a maximum injection time of 50 ms. Monoisotopic peak determination was used, specifying small molecule and an intensity threshold of 2.5×10^4 was used for precursor selection. Data-dependent fragmentation was performed using HCD with a stepped collision energy of 20, 30, and 50 with quadrupole isolation at m/z 1.5 width. The fragment scan resolution using the orbitrap was set at 30,000, ion target value of 5.0×10^4 and 54 ms maximum injection time with the parallelizable option.

LC/-MS Analysis (Non-Polar Extract). Samples were analyzed using a Vanquish UPLC coupled to a Fusion Lumos mass spectrometer (Thermo Fisher Scientific). Samples were reconstituted in 60% acetonitrile in water; 10 mM ammonium formate, 0.1 % formic acid (5 μL) and separated by an Acquity UPLC BEH (1.7 μm , 2.1 mm id x 100 mm length; Waters, Milford MA, USA) C18 column at 300 $\mu\text{L}/\text{min}$ and 45 $^{\circ}\text{C}$ with the gradient program listed in Table 2. The mass spectrometer was operated in positive polarity, default source parameters for the flow rate, and data dependent mode (topN, 1.5 s cycle time) with a dynamic exclusion of 10 s (with 10 ppm error). The RF lens was set at 60 %. Full scan resolution using the orbitrap was set at 120,000 and the mass range was set to m/z 200-1200. Full scan ion target value was 5.0×10^5 allowing a maximum injection time of 50 ms. Monoisotopic peak determination was used, specifying small molecule, and an intensity threshold of 5.0×10^4 was used for precursor selection. Data-dependent fragmentation was performed using HCD with a stepped collision energy of 25, 30, and 35 with quadrupole isolation at m/z 1.6 width. The fragment scan resolution using the orbitrap was set at

15,000, m/z 50 and dynamic maximum injection time. An additional analysis utilizing the same separation method and mass spectrometer settings in negative mode was also performed.

Individual sample extracts were also pooled and acquired in Acquire X data acquisition mode to provide additional MS2 and MS3 data to be used for spectral library matching and annotation. The MS1 method for determining the initial exclusion list from the blank and inclusion list from the sample was run with an orbitrap resolution of 120,000, mass range of m/z 150-1500, and an ion target value of 4.0×10^5 allowing a maximum injection time of 100 ms. For the subsequent DDA runs, the mass spectrometer was operated in positive polarity, default source parameters for the flow rate, and data dependent mode (topN, 1.5 s cycle time) with a dynamic exclusion of 5 s (with 10 ppm error). The RF lens was set at 60 %. Full scan resolution using the orbitrap was set at 120,000 and the mass range was set to m/z 150-1500. Full scan ion target value was 4.0×10^5 allowing a maximum injection time of 100 ms. Monoisotopic peak determination was used, specifying small molecule and an intensity threshold of 5×10^4 was used for precursor selection. Data-dependent fragmentation was performed using HCD with a stepped collision energy of 25, 30, and 35 and quadrupole isolation at m/z 1.6 width. The fragment scan resolution using the orbitrap was set at 15,000, with automated maximum injection time.

During each 1.5 s cycle of the untargeted dd-MS2 profiling method, additional targeted product ion (m/z 184.0733) or neutral loss (fatty acid + NH₃) collisional induced dissociation (CID) MS2 and MS3 experiments were selectively triggered to provide higher quality characterization of phosphatidylcholine (PC) and triglyceride (TG) lipids. CID triggered MS2 scans from parent ions containing an HCD generated MS2 containing m/z 184.0733 fragment, which were collected with a CID collision energy of 32 %, 10 ms activation time, and auto maximum injection time at a resolution of 15,000. Additional MS3 triggered spectra were collected from the three most intense (Top 3 mode) HCD MS2 fragments of a fatty acid and + NH₃ neutral loss from the list (Table 3). A collision energy of 35 %, 10 ms activation time, and auto maximum injection time at 15,000 resolution was used for MS3 spectra collection. An additional analysis utilizing the same separation method and mass spectrometer settings in negative mode was also performed.

LC/MS Data Processing. Resulting raw files were processed and searched with Compound Discoverer (version 3.1) using mzVault (May 2019 mzCloud) NIST20, curated mass lists. The following search parameters were used for Compound Discoverer searches: Retention time alignment was used with an adaptive curve model and 2 min maximum shift with 8 ppm mass tolerance. The detect compounds node was set to a mass tolerance of 8 ppm, intensity tolerance of 30 %, S/N threshold of 3, minimum peak intensity of 50,000, base ions of [M+H]⁺+1, [M-H]⁻-1, minimum element count C H and maximum element count of C100 H190 Br3 Cl4 K2 N10 Na2 O15 P3 S5, and constant mean normalization was used for statistical data processing. The assign compound annotation node was used with 8 ppm mass tolerance with mzVault, predicted compounds, and mass list search. All library searches of mzVault included a mass tolerance of 10 ppm of precursor and product ions and maximum retention time shift of 2 min after alignment with the HighChem-HighRes algorithm. Local mass list (LipidMaps, EFS HRAM Compound Database, Endogenous Metabolite Database and Extractables and Leachables HRAM Database) were searched with a mass tolerance of 8 ppm. Total mass features were reduced, background

features filtered from the final analysis, and results exported in .csv format for further data comparison.

4.2. Results and Discussion

Untargeted metabolomics was performed on the polar and non-polar sample extracts and subjected to unsupervised chemometric analysis. The principal component analysis (PCA) scores plot of the polar extract analyzed in positive and negative mode are shown in (Figure 6). The scores plot distinguishes each cohort- vegan and omnivore diets, regardless of preservation method. The PCA scores plot of the non-polar extract analyzed in positive and negative mode is shown in (Figure 7).

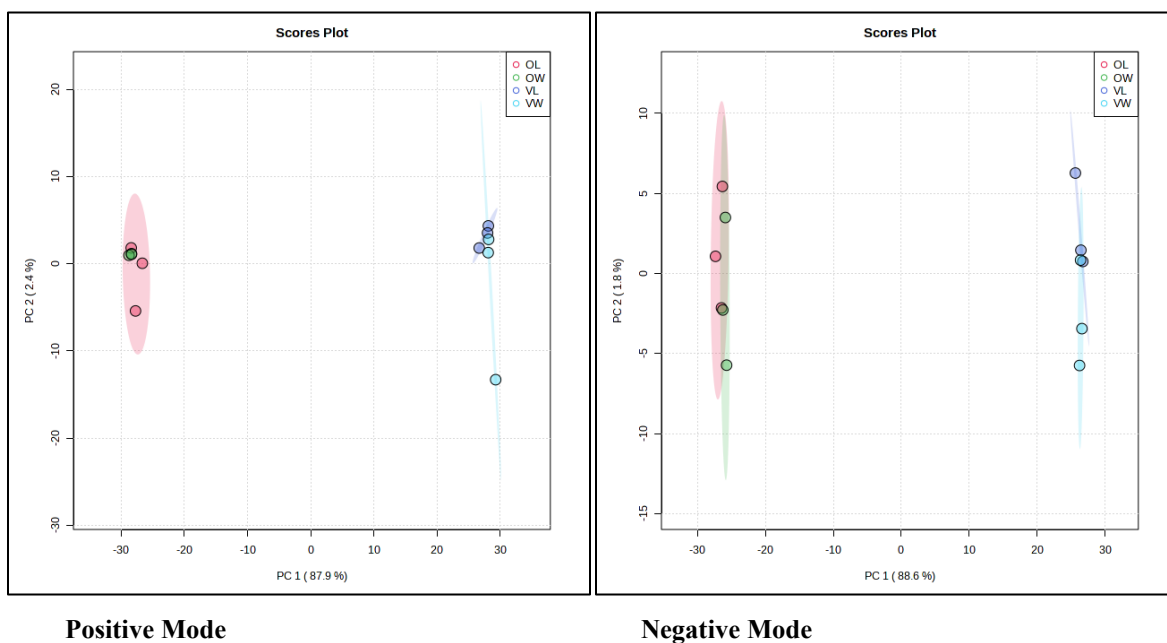


Figure 6. Principal component analysis scores plot (PC1 vs. PC2) of polar sample extracts from omnivore aqueous (OA), omnivore lyophilized (OL), vegan aqueous (VA), and vegan lyophilized (VL). The ellipses indicate the 95% confidence interval.

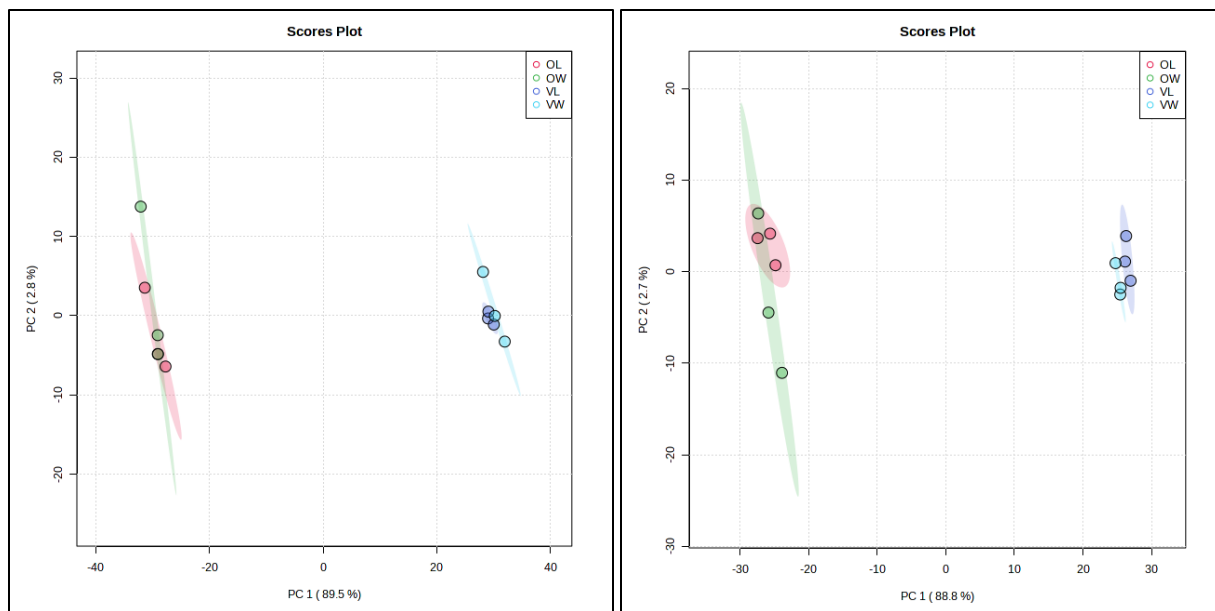


Figure 7. Principal component analysis scores plot (PC1 vs PC2) of non-polar sample extracts from omnivore aqueous (OA), omnivore lyophilized (OL), vegan aqueous (VA), and vegan lyophilized (VL). The ellipses indicate the 95% confidence interval.

The acquired HCD MS2 mass spectra were matched to the spectral libraries as described above for compound annotation purposes. Tables 1-4 lists the top 20 metabolites for each sample type in order of abundance for the respective extract and polarity mode. Due to ion suppression that may occur during electrospray ionization, these most abundant metabolites may not be representative of the most concentrated metabolites in the samples.

Table 2. Top 20 most abundant metabolites by LC-HRMS for each sample type as identified by MS/MS spectral library. (Polar extract – **positive mode**). Metabolites observed in the same order across all samples (green), metabolites observed across all samples, but order is inconsistent (yellow), metabolites observed across some samples (blue) and metabolites only observed in one sample (pinkish-orange).

Vegan Lyophilized	Vegan Aqueous	Omnivore Lyophilized	Omnivore Aqueous
Stercobilin	Stercobilin	Stercobilin	Stercobilin
PEG n8	PEG n8	Phenylacetaldehyde	Phenylacetaldehyde
Phenylacetaldehyde	Phenylacetaldehyde	Hypoxanthine	Hypoxanthine
Hypoxanthine	PEG n10	L-Tryptophan	L-Tryptophan
PEG n11	PEG n11	N-Acetyl-D-tryptophan	N-Acetyl-D-tryptophan
PEG n10	(2S)-2-Hydroxy-2-phenylpropanoic acid	(2S)-2-Hydroxy-2-phenylpropanoic acid	L-Norleucine
L-Tryptophan	Hypoxanthine	L-Norleucine	(2S)-2-Hydroxy-2-phenylpropanoic acid
N-Acetyl-D-tryptophan	L-Norleucine	L-Tyrosine	L-Tyrosine
(2S)-2-Hydroxy-2-phenylpropanoic acid	L-Tryptophan	L-Methionine	L-Methionine
L-Norleucine	N-Acetyl-D-tryptophan	Pregabalin	Pregabalin
L-Tyrosine	PEG n7	3-Acetoxy pyridine	3-Acetoxy pyridine
PEG n7	Pregabalin	L-Glutamic acid	2-Butenoic acid, 2-ethyl-, (Z)-
L-Methionine	L-Tyrosine	2-Butenoic acid, 2-ethyl-, (Z)-	L-Glutamic acid
Pregabalin	Glycodeoxycholic acid	Urocanic acid	Urocanic acid
L-Glutamic acid	L-Methionine	DL-o-Tyrosine	Nicotinic acid
Xanthine	β -Hyodeoxycholic acid	Nicotinic acid	DL-o-Tyrosine
2-Butenoic acid, 2-ethyl-, (Z)-	L-Glutamic acid	Xanthine	Methyl 4-hydroxycinnamate
Glycodeoxycholic acid	2-Butenoic acid, 2-ethyl-, (Z)-	Methyl 4-hydroxycinnamate	Xanthine
β -Hyodeoxycholic acid	Xanthine	1-Acetyl piperidine-2-carboxylic acid	Acetylcholine
DL-o-Tyrosine	DL-o-Tyrosine	Valine	1-Acetyl piperidine-2-carboxylic acid

Table 3. Top 20 most abundant metabolites by LC-HRMS for each sample type as identified by MS/MS spectral library matching (Polar extract – **negative mode**). Metabolites observed in the same order across all samples (green), metabolites observed across all samples, but order is inconsistent (yellow), metabolites observed across some samples (blue) and metabolites only observed in one sample (pinkish-orange).

Vegan Lyophilized	Vegan Aqueous	Omnivore Lyophilized	Omnivore Aqueous
Sucralose	Sucralose	5-Hydroxy-2,2,6,6-tetramethyl-4-[3-methyl-1-[2,4,6-trihydroxy-3-(2-methylpropanoyl)phenyl]butyl]cyclohex-4-ene-1,3-dione	5-Hydroxy-2,2,6,6-tetramethyl-4-[3-methyl-1-[2,4,6-trihydroxy-3-(2-methylpropanoyl)phenyl]butyl]cyclohex-4-ene-1,3-dione
4-Acetyloxy-6-hydroxy-2-(2-hydroxypropan-2-yl)-4a,6-dimethyl-3,4,5,7,8,8a-hexahydro-2H-chromene-5-carboxylic acid	4-Acetyloxy-6-hydroxy-2-(2-hydroxypropan-2-yl)-4a,6-dimethyl-3,4,5,7,8,8a-hexahydro-2H-chromene-5-carboxylic acid	L(-)-Malic acid	(2,5-Dioxotetrahydrofuran-3-yl)acetic acid
(2,5-Dioxotetrahydrofuran-3-yl)acetic acid	(2,5-Dioxotetrahydrofuran-3-yl)acetic acid	(2,5-Dioxotetrahydrofuran-3-yl)acetic acid	Xanthine
3-Sulfopropanoic acid	L(-)-Malic acid	Xanthine	L(-)-Malic acid
L(-)-Malic acid	1-O-((2E,4E)-9-Carboxy-8-hydroxy-2,7-dimethylnona-2,4-dienoyl)-β-D-glucopyranose	3-Hydroxykynurenine	3-Hydroxykynurenine
4-Oxododecanedioic acid	3-Sulfopropanoic acid	5-Phenylisoxazol-3-ol	Deoxycholic acid
Deoxycholic acid	Deoxycholic acid	Deoxycholic acid	5-Phenylisoxazol-3-ol
3,3-Dimethylglutaric acid	4-Oxododecanedioic acid	1-O-((2E,4E)-9-Carboxy-8-hydroxy-2,7-dimethylnona-2,4-dienoyl)-β-D-glucopyranose	1-O-((2E,4E)-9-Carboxy-8-hydroxy-2,7-dimethylnona-2,4-dienoyl)-β-D-glucopyranose
Xanthine	3,3-Dimethylglutaric acid	4-Oxododecanedioic acid	4-Oxododecanedioic acid
1-O-((2E,4E)-9-Carboxy-8-hydroxy-2,7-dimethylnona-2,4-dienoyl)-β-D-glucopyranose	Xanthine	4-Acetyloxy-6-hydroxy-2-(2-hydroxypropan-2-yl)-4a,6-dimethyl-3,4,5,7,8,8a-hexahydro-2H-chromene-5-carboxylic acid	4-Acetyloxy-6-hydroxy-2-(2-hydroxypropan-2-yl)-4a,6-dimethyl-3,4,5,7,8,8a-hexahydro-2H-chromene-5-carboxylic acid
5-Hydroxy-2,2,6,6-tetramethyl-4-[3-methyl-1-[2,4,6-trihydroxy-3-(2-methylpropanoyl)phenyl]butyl]cyclohex-4-ene-1,3-dione	Azelaic acid	L-Glutamic acid	L-Glutamic acid
Azelaic acid	5-Hydroxy-2,2,6,6-tetramethyl-4-[3-methyl-1-[2,4,6-trihydroxy-3-(2-methylpropanoyl)phenyl]	Adipic acid	3,3-Dimethylglutaric acid

	butyl]cyclohex-4-ene-1,3-dione		
L-Glutamic acid	L-Glutamic acid	Hypoxanthine	Glutaric acid
Hypoxanthine	Hypoxanthine	3,3-Dimethylglutaric acid	Hypoxanthine
Auriculatin	Auriculatin	Scopolamine .beta.-D-glucuronide	Adipic acid
trans-Traumatic acid	trans-Traumatic acid	3-Sulfopropanoic acid	3-Sulfopropanoic acid
5-Phenylisoxazol-3-ol	Suberic acid	16-Hydroxyhexadecanoic acid	Scopolamine .beta.-D-glucuronide
Suberic acid	2,4-Bis(4-hydroxyphenyl)cyclobutane-1,3-dicarboxylic acid	Glutaric acid	16-Hydroxyhexadecanoic acid
2,4-Bis(4-hydroxyphenyl)cyclobutane-1,3-dicarboxylic acid	Uric acid	2,4-Bis(4-hydroxyphenyl)cyclobutane-1,3-dicarboxylic acid	2,4-Bis(4-hydroxyphenyl)cyclobutane-1,3-dicarboxylic acid
Uric acid	3-Hydroxykynurenine	Quinolin-2-ol	Pantothenic acid

Table 4. Top 20 most abundant metabolites by LC-HRMS for each sample type as identified by MS/MS spectral library matching (**Non-polar extract** – positive mode). Metabolites observed in the same order across all samples (green), metabolites observed across all samples, but order is inconsistent (yellow), metabolites observed across some samples (blue) and metabolites only observed in one sample (pinkish-orange).

Vegan Lyophilized	Vegan Aqueous	Omnivore Lyophilized	Omnivore Aqueous
Stercobilin	Stercobilin	Stercobilin	Stercobilin
PEG n11	PEG n11	2-Arachidonoylglycerol	Piperine
PEG n12	PEG n12	7 β ,17 α -Dimethyl-5 β -androsterane-3 α ,17 β -diol	2-Arachidonoylglycerol
PEG n10	PEG n10	ω -3 Arachidonic acid methyl ester	ω -3 Arachidonic acid methyl ester
PEG n13	Piperine	Urobilin	7 β ,17 α -Dimethyl-5 β -androsterane-3 α ,17 β -diol
Piperine	PEG n13	Monoelaidin	5 α -Pregn-2-en-20-one
PEG n8	PEG n8	Dihomo- γ -linolenic acid methyl ester	Monoelaidin
PEG n15	PEG n15	5 α -Pregn-2-en-20-one	Dihomo- γ -linolenic acid methyl ester
Urobilin	Urobilin	1-Oleoyl-2-acetyl-sn-glycerol	Urobilin
PEG n16	PEG n16	Piperine	1-Oleoyl-2-acetyl-sn-glycerol
5-Fluoro ADBICA	Pheophorbide a	3-(β -D-Galactopyranosyloxy)-2-hydroxypropyl (9Z,12Z)-octadeca-9,12-dienoate	3-(β -D-Galactopyranosyloxy)-2-hydroxypropyl (9Z,12Z)-octadeca-9,12-dienoate
Pheophorbide a	D- α -Tocopherol succinate	17-(1-Hydroxyethyl)-10,13-dimethyl-2,3,6,7,8,9,10,11,12,13,14,15,16,17-tetradecahydro-1H-cyclopenta[a]21henanthrene-3-one	3-[[Cholamidopropyl]dimethylammonio]-1-propanesulfonate
D- α -Tocopherol succinate	5-Fluoro ADBICA	Methasterone	Methasterone
3-[[Cholamidopropyl]dimethylammonio]-1-propanesulfonate	2-Arachidonoylglycerol	Heneicosapentaenoic acid	5 β -Pregnane-3 α ,17 α ,21-triol-20-one
2-Arachidonoylglycerol	3-[[Cholamidopropyl]dimethylammonio]-1-propanesulfonate	3-[[Cholamidopropyl]dimethylammonio]-1-propanesulfonate	9,11-Methane-epoxyprostaglandin F1 α
PEG n7	Guineensine	5 β -Pregnane-3 α ,17 α ,20 α -triol	5 β -Pregnane-3 α ,17 α ,20 α -triol
1-Oleoyl-2-acetyl-sn-glycerol	PEG n7	Misoprostol	Misoprostol
Guineensine	1-Oleoyl-2-acetyl-sn-glycerol	9,11-Methane-epoxyprostaglandin F1 α	17-(1-Hydroxyethyl)-10,13-dimethyl-2,3,6,7,8,9,10,11,12,13,14,15,16,17-tetradecahydro-

			1H-cyclopenta[a]22henanthrene-3-one
Methyl jasmonate	7 β ,17 α -Dimethyl-5 β -androstane-3 α ,17 β -diol	5 β -Pregnane-3 α ,17 α ,21-triol-20-one	(+)-Aphidicolin
7 β ,17 α -Dimethyl-5 β -androstane-3 α ,17 β -diol	Methyl jasmonate	(5Z,9E)-4-Hydroxy-1,5,9-trimethyl-12-(propan-2-yl)-15-oxabicyclo[10.2.1]pentadeca-5,9-dien-2-yl acetate	PEG n15

Table 5. Top 20 most abundant metabolites by LC-HRMS for each sample type as identified by MS/MS spectral library matching (**Non-polar extract** – negative mode). Metabolites observed in the same order across all samples (green), metabolites observed across all samples, but order is inconsistent (yellow), metabolites observed across some samples (blue) and metabolites only observed in one sample (pinkish-orange).

Vegan Lyophilized	Vegan Aqueous	Omnivore Lyophilized	Omnivore Aqueous
3-Oxostearic acid	3-Oxostearic acid	3-Oxostearic acid	3-Oxostearic acid
Linoleic acid	Linoleic acid	(Z)-6-Octadecenoic acid	(Z)-6-Octadecenoic acid
Pinolenic acid	(Z)-6-Octadecenoic acid	Linoleic acid	Linoleic acid
(Z)-6-Octadecenoic acid	trans-Traumatic acid	16-Hydroxyhexadecanoic acid	Ricinoleic acid
Ricinoleic acid	Ricinoleic acid	Ricinoleic acid	16-Hydroxyhexadecanoic acid
1-(3,4-Dihydroxyphenyl)-7-(4-hydroxyphenyl)-4-hepten-3-one	Pinolenic acid	1,7-Dihydroxyxanthone	1,7-Dihydroxyxanthone
(15:3)-Anacardic acid	(15:3)-Anacardic acid	1-Palmitoyl-2-hydroxy-sn-glycero-3-phosphoethanolamine	Acerogenin G
trans-Traumatic acid	1-(3,4-Dihydroxyphenyl)-7-(4-hydroxyphenyl)-4-hepten-3-one	Acerogenin G	1-Palmitoyl-2-hydroxy-sn-glycero-3-phosphoethanolamine
1,7-Dihydroxyxanthone	Ginkgolic acid I	2-Hydroxypalmitic acid	9,10-Dihydroxy-12Z-octadecenoic acid
Ginkgolic acid I	(6E,10Z,14E)-6,14-Dimethyl-3-methylidene-2-oxo-3a,4,5,8,9,12,13,15a-octahydrocyclo[10.2.1]pentadeca[b]furan-10-carboxylic acid	(6E,10Z,14E)-6,14-Dimethyl-3-methylidene-2-oxo-3a,4,5,8,9,12,13,15a-octahydrocyclo[10.2.1]pentadeca[b]furan-10-carboxylic acid	1-(1Z-Octadecenyl)-2-(4Z,7Z,10Z,13Z,16Z,19Z-docosahexaenyl)-sn-glycero-3-phosphoethanolamine
4-Deoxyphloridzin	1,7-Dihydroxyxanthone	Pinolenic acid	(6E,10Z,14E)-6,14-Dimethyl-3-methylidene-2-oxo-3a,4,5,8,9,12,13,15a-octahydrocyclo[10.2.1]pentadeca[b]furan-10-carboxylic acid
DL- α -Tocopherol	4-Deoxyphloridzin	1-(1Z-Octadecenyl)-2-(4Z,7Z,10Z,13Z,16Z,19Z-docosahexaenyl)-sn-	2-Hydroxypalmitic acid

		glycero-3-phosphoethanolamine	
(6E,10Z,14E)-6,14-Dimethyl-3-methylidene-2-oxo-3a,4,5,8,9,12,13,15a-octahydrocyclootetradeca[b]furan-10-carboxylic acid	(10E,15Z)-9,12,13-Trihydroxyoctadeca-10,15-dienoic acid	12,13-Dihydroxy-9Z-octadecenoic acid	12,13-Dihydroxy-9Z-octadecenoic acid
(10E,15Z)-9,12,13-Trihydroxyoctadeca-10,15-dienoic acid	1-Palmitoyl-2-hydroxy-sn-glycero-3-phosphoethanolamine	9,10-Dihydroxy-12Z-octadecenoic acid	Pinolenic acid
1-Palmitoyl-2-hydroxy-sn-glycero-3-phosphoethanolamine	DL- α -Tocopherol	Aceroside VII	Aceroside VII
13-Keto-9Z,11E-octadecadienoic acid	13-Keto-9Z,11E-octadecadienoic acid	4-Deoxyphloridzin	13-Keto-9Z,11E-octadecadienoic acid
12,13-Dihydroxy-9Z-octadecenoic acid	Isorosmanol	9-Hydroperoxy-10E,12Z,15Z-octadecatrienoic acid	4-Deoxyphloridzin
9,10-Dihydroxy-12Z-octadecenoic acid	12,13-Dihydroxy-9Z-octadecenoic acid	13-Keto-9Z,11E-octadecadienoic acid	9-Hydroperoxy-10E,12Z,15Z-octadecatrienoic acid
(Z)-6,9,10-Trihydroxyoctadec-7-enoic acid	(Z)-6,9,10-Trihydroxyoctadec-7-enoic acid	12(13)-Epoxy-9Z-octadecenoic acid	12(13)-Epoxy-9Z-octadecenoic acid
12-Methoxycarnosic acid	9,10-Dihydroxy-12Z-octadecenoic acid	Bilirubin	Carbocyclic thromboxane A ₂

5. Stool Characterization via GC-MS

5.1. Methods

Sample Preparation for GCxGC-TOFMS Analysis. Samples were transferred to 20 mL glass headspace sample vial and sealed with a septum cap. All analyses were performed in triplicate. The solid phase micro extraction was conducted at 60 °C for 30 min with a 2 cm, 50/30 µm, divinylbenzene/carboxen/polydimethyl- siloxane SPME. Fiber desorption (90 s at 270 °C) and sample injection followed immediately after headspace SPME extraction. A split injection of 10:1 was used for this analysis.

GCxGC-TOFMS Analysis. The samples were analyzed for volatile organics using comprehensive two-dimensional gas chromatography coupled to a time-of-flight mass spectrometer (LECO Pegasus 4D GCxGC-TOFMS). The separation was performed using a 30 m × 0.25 µm ID × 1.4 µm df Rxi-624SilMS column in the first dimension followed by a 1.75 m × 0.25 µm ID × 0.25 µm df StabilWAX column in the second dimension using He as carrier gas at 1.0 mL/min. The GC oven was held at 40 °C for 0.2 min followed by a 5 °C/min ramp to 240 °C. The secondary GC oven was offset by 5 °C, while the modulator was offset by 15 °C from the primary GC oven. A modulation time of 3.0 s was used. The TOFMS was operated from 35 to 550 m/z at -70 eV at an acquisition frequency of 200 Hz. The mass spectra were library searched using the NIST20 mainlib and replib libraries. A spectral similarity of 700 out of a possible 1000 was required before an annotation was assigned.

5.2. Results and Discussion

The analysis of volatile metabolites by GCxGC-TOFMS revealed differences between the lyophilized and aqueous samples. As highlighted in the GCxGC total ion chromatograms (**Figure 8**), the short chain fatty acids appear elevated in the lyophilized samples. While initially this finding may be counter intuitive, as many believe that the volatility of short chain fatty acids would result in losses during the lyophilization process, the the lyophilized material may have contributed to a higher desorption efficiency during SPME process.

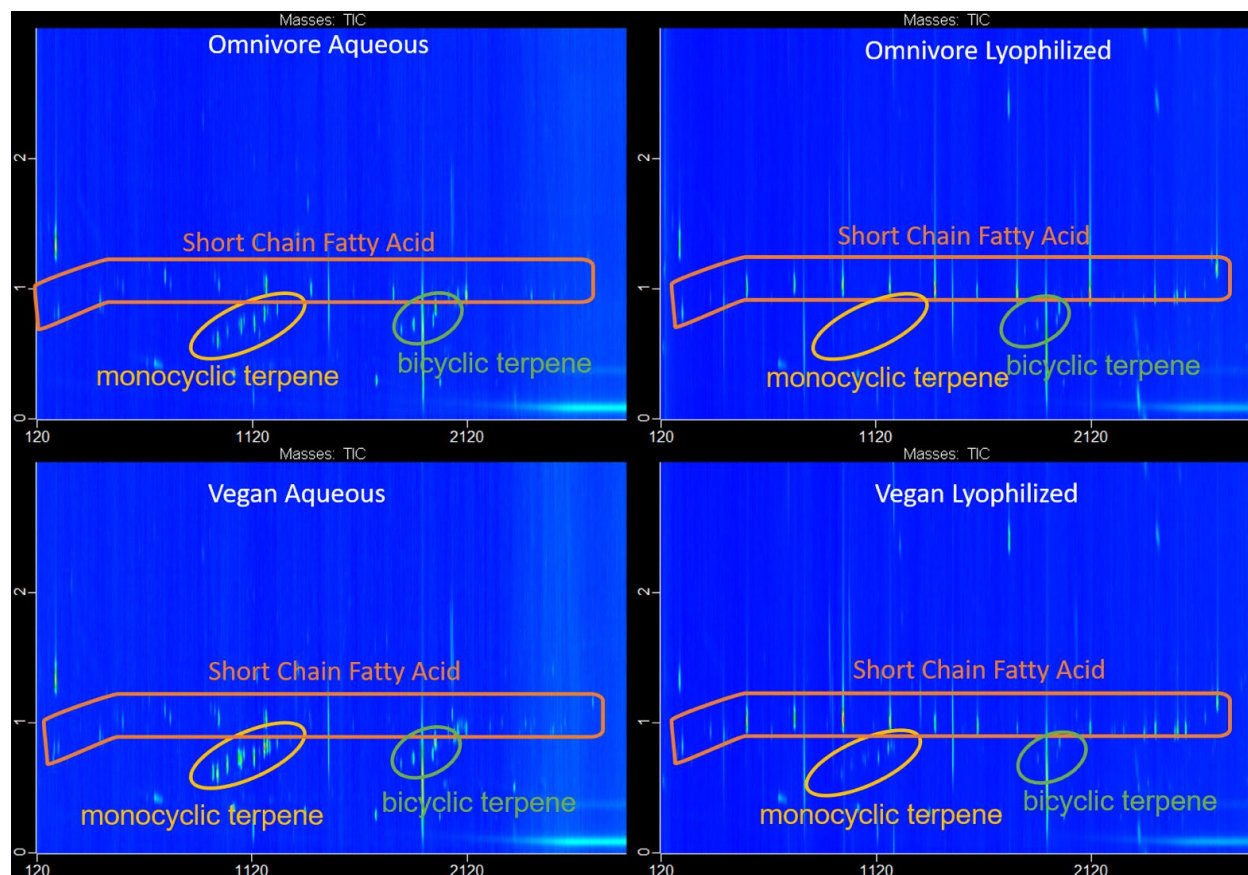


Figure 8. The GCxGC-TOFMS total ion chromatograms for omnivore aqueous, omnivore lyophilized, vegan aqueous, and vegan lyophilized samples.

Another class of compounds that are of interest are terpenes. Differences between the vegan and omnivore samples, and material preparation were observed in the volatile metabolite analysis. As expected, vegan samples showed elevated levels of monocyclic terpene, which would correlate to a greater dietary intake of plant material. When comparing terpenes in lyophilized and aqueous samples, the relative abundance of terpenes is greater in the aqueous samples, indicating that lyophilization may lead to losses of these compounds. Alternatively, competitive sorption to the SPME fiber by the short chain fatty acids may outcompete terpenes, thus biasing the analysis. Static headspace measurements could be employed to determine if this bias is being introduced during the SPME analysis.

Relative-quantitative analysis was performed by comparing the mass spectral area of the detected compounds to that of the area of indole-d6, the internal standard. The top 20 metabolites based on the calculated relative abundance results are reported in **Table 6**. Top 20 metabolites based on relative abundance detected and identified by GCxGC-TOFMS. The table describes metabolites observed in the same order across all samples (green), metabolites observed across all samples, but order is inconsistent (yellow), metabolites observed across some samples (blue) and metabolites only observed in one sample (pinkish-orange).

Table 6. Top 20 metabolites based on relative abundance detected and identified by GCxGC-TOFMS. The table describes metabolites observed in the same order across all samples (green), metabolites observed across all samples, but order is inconsistent (yellow), metabolites observed across some samples (blue) and metabolites only observed in one sample (pinkish-orange).

Vegan Lyophilized	Vegan Aqueous	Omnivore Aqueous	Omnivore Lyophilized
Hexanoic acid, methyl ester	Isopropyl Alcohol	Isopropyl Alcohol	Dodecanoic acid, methyl ester
Isopropyl Alcohol	p-Cresol	Dodecanoic acid, methyl ester	Octanoic acid, methyl ester
Butanoic acid, methyl ester	Indole	o-Cymene	Decanoic acid, methyl ester
Heptanoic acid, methyl ester	Limonene	p-Cresol	Isopropyl Alcohol
Methyl valerate	Sabinene	Indole	Hexanoic acid, methyl ester
Butanoic acid	trans- β -Ocimene	Acetic acid, methyl ester	Hexadecanoic acid, methyl ester
Hexadecanoic acid, methyl ester	α -Pinene	Octanoic acid, methyl ester	Heptanoic acid, methyl ester
p-Cresol	o-Cymene	Decanoic acid, methyl ester	Acetic acid, methyl ester
Acetic acid, methyl ester	(-)- β -Pinene	α -Pinene	Methyl tetradecanoate
Octanoic acid, methyl ester	Indole, 3-methyl-	trans- β -Ocimene	Butanoic acid
Nonanoic acid, methyl ester	Acetic acid, methyl ester	(-)- β -Pinene	Butanoic acid, methyl ester
Dodecanoic acid, methyl ester	Camphene	Limonene	p-Cresol
Methyl tetradecanoate	β -Thujene	Caryophyllene	Methyl valerate
Tetradecanoic acid, 12-methyl-, methyl ester	Hexanoic acid, methyl ester	Indole, 3-methyl-	Indole

Hexanoic acid	Caryophyllene	γ -Terpinene	Nonanoic acid, methyl ester
Indole	Benzaldehyde	Hexanoic acid, methyl ester	Ethanol
Methyl propionate	Eucalyptol	2-Norpinene	Tetradecanoic acid, 12-methyl-, methyl ester
Methyl stearate	Copaene	Butanal, 3-methyl-	Hexanoic acid
Pentadecanoic acid, methyl ester	Butanoic acid	Copaene	Boric acid, trimethyl ester
Indole, 3-methyl-	2-Norpinene	Hexadecanoic acid, methyl ester	Methyl stearate

6. Stool Characterization via ^1H NMR

6.1. Methods

Sample Preparation. Four vials from each RGTM were analyzed to give a total of 16 samples. For the lyophilized samples (equivalent to 100 mg of wet material), 800 μL of deuterium oxide (D_2O) was added directly to the sample vial. The sample was dispersed in solution by vortexing for 1 min (in 15 s intervals) then transferred with the aid of a pipette to a 1.5 mL microfuge tube. The sample was vortexed again for 1 min after transferring. Insoluble debris in the sample was removed by centrifugation at 10,000 \times g for 5 min at room temperature. The supernatant was filtered by using a 10 mL syringe connected to a 0.2 μm syringe filter. The filtrate was transferred to a 0.1 μm centrifugal filter and centrifuged for 15 min at 15,000 \times g at 16 $^\circ\text{C}$. The NMR sample was prepared by placing 450 μL of the final filtrate and 150 μL of D_2O -phosphate buffer in a microfuge tube, vortexing for 10 s, then transferring to a 5 mm NMR tube. The D_2O -phosphate buffer was prepared by mixing 1.0647 g disodium phosphate (Na_2HPO_4), (#S5136-100G, Sigma) and 0.3564 g monosodium phosphate (NaH_2PO_4), (#S0751-100G, Sigma) to make 100 mL buffer (pH = 7.2) to which 80 mg sodium-3-trimethylsilylpropionate (TMSP), (#DLM48-1, Cambridge Isotope Laboratories, Inc.) was added as an internal standard.

For the aqueous stool RGTMs stored at -80 $^\circ\text{C}$, sample processing only differed from the lyophilized preparation in the first step: D_2O was not added to the samples prior to filtration as they were already dispersed in water prior to packaging. Aqueous stool samples were thawed at room temperature for 30 min. Thawed samples were stored on ice prior to handling.

NMR Analysis. ^1H NMR spectra were acquired at 298 K on a Bruker Avance II 600 MHz NMR spectrometer equipped with a room temperature broadband inverse probe. Spectra were acquired with a nuclear Overhauser effect spectroscopy (NOESY) water presaturation sequence (Bruker noesygppr1d) with the following acquisition parameters: 8 dummy scans, 64 scans, 32768 complex data points, 10 s relaxation delay and 20.02 ppm spectral width. Total acquisition time per spectrum was approximately 14 min. FIDs were zero filled to 65536 points prior to Fourier transform. No significant interferences from macromolecules were observed in the spectra so additional measures, such as T2 filtering (e.g. CPMG sequence), were deemed unnecessary. The chemical shift axis was calibrated by setting the TMSP peak to 0 ppm. Spectra were referenced and manually phase corrected using Topspin version 3.6.5. Mnova (Version 14.1.2, Mestrelab Research) was used for spectra visualization and plotting. Deconvolution of the NMR peaks for identification and quantification of metabolites was performed using the Chenomx NMR Suite (Ver 8.6, Chenomx Inc, Edmonton, Canada). TMSP concentration was used as internal standard to obtain the metabolites concentration. Comparison across different diets and storage conditions was conducted using the derived concentration lists.

6.2. Results and Discussion

^1H NMR was used in this study to identify and quantify hydrophilic metabolites (measurand) in a ranking manner. The measurand concentration was obtained relative to the concentration of the internal standard TMSP (**Appendix C**). ^1H NMR spectra for each stool material: vegan diet stored in aqueous phase (Vegan-Aq), lyophilized vegan diet (Vegan-Ly), omnivore diet stored in aqueous phase (Omni-Aq) and lyophilized omnivore diet (Omni-Ly) are displayed in **Figure 9**.

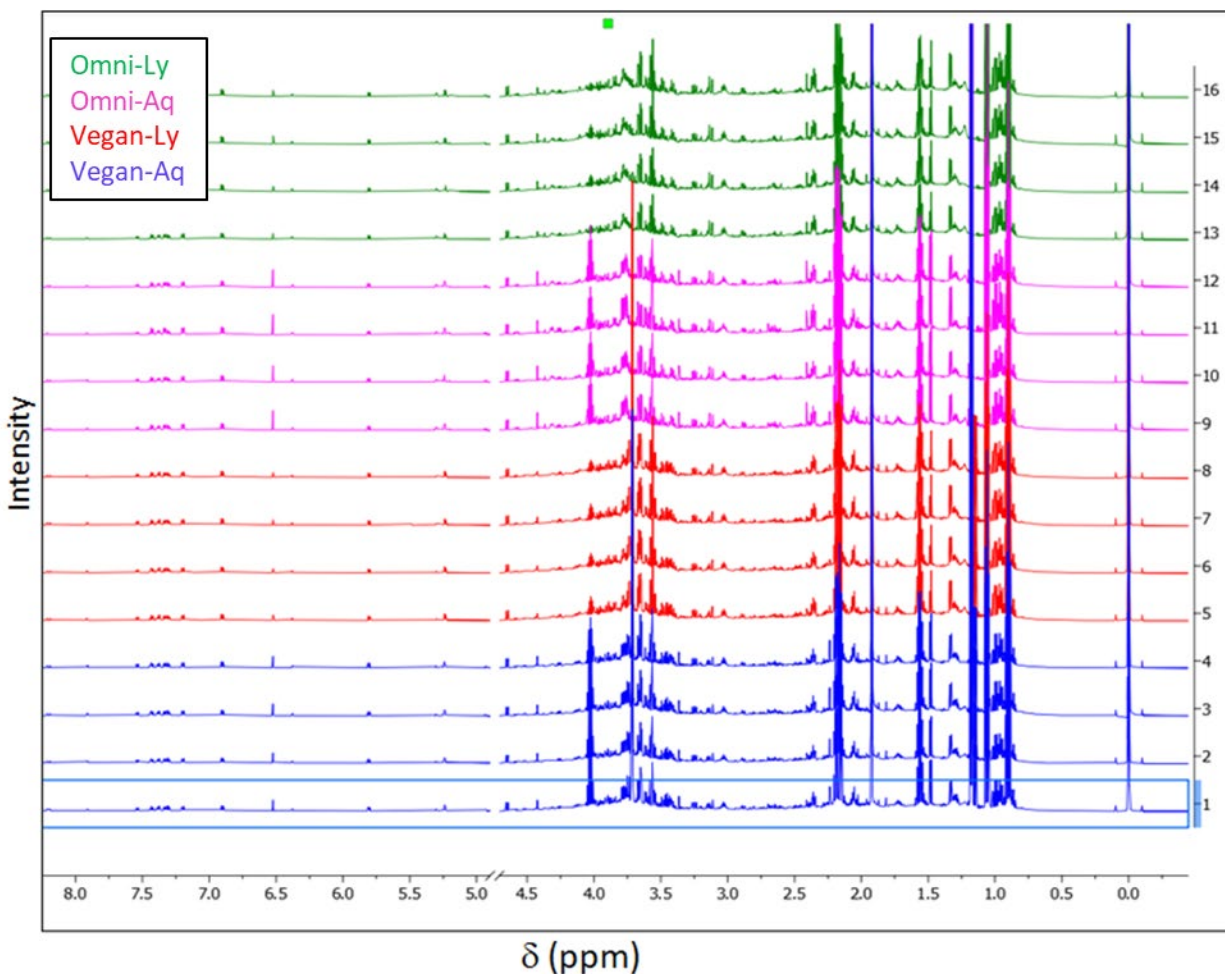


Figure 9. NMR spectra of human stool samples.

A total of 45 compounds were identified across all stool samples (Vegan-Aq, Vegan-Ly, Omni-Ly and Omni-Ly) (**Figure 10**). Some of these compounds are of clinical and health relevance [8] and have been described in the fecal metabolome database [9]. Most of the identified compounds were observed across all samples with a few exceptions, e.g. 2-methylglurate was detected only in lyophilized samples (vegan and omnivore) (**Figure 10**). A comparison between diets revealed that vial-to-vial variability appeared to be higher among omnivore samples compared to vegan samples across all metabolites. Vegan-Aq had 4 out of 45 metabolites above 20 % RSD (8.9%), vegan-ly had 12 out of 45 (27%), omni-ly had 33 out of 45 (73%) and omni-aq had 29 out of 45 (64%) (**Appendix C**).

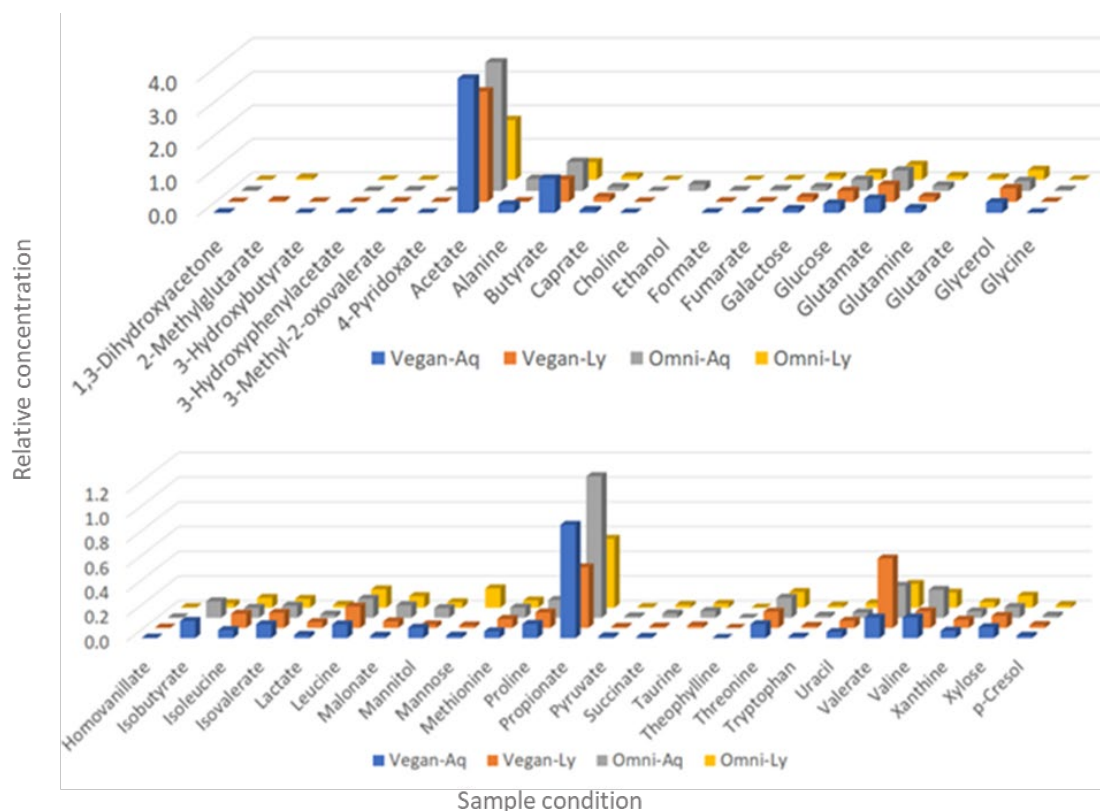


Figure 10. Relative concentrations of the 45 compounds identified from ^1H NMR spectra across the stool materials. Four vials were analyzed ($n = 4$) for each stool material.

Variance in measured metabolite concentrations may increase in response to NMR sample stability, extraction reproducibility, low metabolite concentration or inhomogeneity across material replicates. Human stool is a complex material that contains a variety of biologically active components, including human cells (colonocytes), microbiota and diverse dietary products [10]. The enzymatic activity of digestive, bacterial, and dietary components adds to this complexity. In this regard, sample handling and preparation for metabolomics studies require critical consideration to maintain the integrity of the original sample by minimizing enzymatic activity. There are approaches to minimize the impact of enzymatic activity on the stability of the sample and the extracted metabolites including the use of an organic solvent to quench enzymatic activity (protein denaturation and precipitation) in metabolomics workflows, keeping samples and extraction solvents cold to reduce enzymatic activity, and the use of sodium azide to stabilize the metabolite extract from potential microbial growth [11].

During sample preparation, the omnivore samples exhibited a layer of hydrophobic compounds floating on the surface of the supernatant after centrifugation (**Figure 11**). This layer was not observed on vegan samples and is likely related to diet.

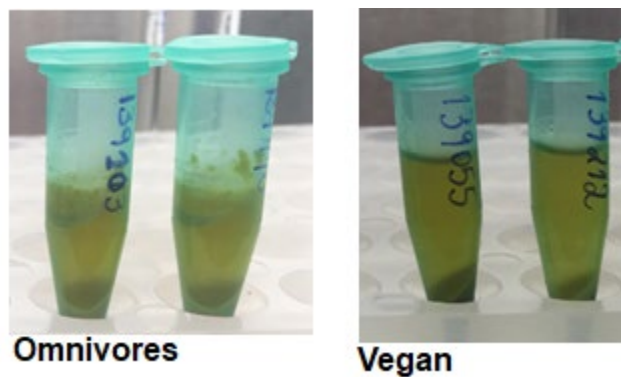


Figure 11. Physical characteristic of the stool samples extracted in water after centrifugation for removal of debris.

The 20 most abundant metabolites determined by ^1H NMR were composed mostly of short chain fatty acids (SCFAs) and amino acids including branched ones (**Table 7**). Acetate was the most abundant compound in all materials. Butyrate, propionate, and glutamate were also in the top 5 metabolites in each material. Observed compounds varied in concentration across different stool materials (data not shown).

Table 7. Top 20 metabolites per stool material obtained via ¹H NMR. The table describes metabolites observed in the same order across all samples (green), metabolites observed across all samples, but order is inconsistent (yellow), metabolites observed across some samples (blue) and metabolites only observed in one sample (pinkish-orange).

Vegan Lyophilized	Vegan Aqueous	Omnivore Lyophilized	Omnivore Aqueous
Acetate	Acetate	Acetate	Acetate
Butyrate	Butyrate	Propionate	Propionate
Valerate	Propionate	Butyrate	Butyrate
Glutamate	Glutamate	Glutamate	Glutamate
Propionate	Glycerol	Glycerol	Alanine
Glycerol	Glucose	Glucose	Glucose
Glucose	Alanine	Valerate	Glycerol
Leucine	Valine	Mannose	Valerate
Glutamine	Valerate	Leucine	Valine
Caprate	Isobutyrate	Threonine	Ethanol
Galactose	Glutamine	Valine	Threonine
Valine	Proline	Glutamine	Glutamine
Threonine	Threonine	Galactose	Leucine
Proline	Isovalerate	Caprate	Proline
Isovalerate	Leucine	Xylose	Isobutyrate
Isoleucine	Galactose	Malonate	Galactose
Xylose	Xylose	Isoleucine	Caprate
Methionine	Mannitol	Isovalerate	Malonate
Xanthine	Caprate	2-Methylglutarate	Isovalerate
Uracil	Isoleucine	Glutarate	Xylose

7. Conclusion

These RGTMs were used to look at the effect of different preservation methods, to optimize protocols, and to evaluate the utility of diet as a distinguishing factor for 2 cohorts. Overall we found all three metabolomics techniques and metagenomics revealed differences between diet cohorts. Different preservation methods introduced some inconsistencies between materials. Therefore, we proposed to move forward with a single preservation method, aqueous, as this is most similar to methods currently being used in the field.

NIST scientists were able to participate in the RGTm production workflow. Notably, this experience emphasized the importance of examining each manipulation on the fecal sample, from collection to storage of the final aliquots, as a critical step for identifying potential places where variability may be introduced and affect homogeneity of the final material. A preliminary characterization of each RGTm was carried out using both metagenomic and metabolomic techniques. These techniques were chosen to evaluate fitness-for-purpose as they represent the primary use cases.

Metagenomic analysis was conducted at the genus and phyla level, to balance the ability to accurately assign a taxonomy and provide the most useful information to the end user. With respect to metagenomic measurement, the establishment of a limit of detection will be necessary for determining homogeneity and stability. Taken as a whole, the data suggest we can produce a homogenous fecal reference material; however, genera present at a low relative abundance ($\leq 0.3\%$) may not appear consistently in all aliquots. These inconsistencies could be due to the measurement workflow or reflect actual differences in the aliquots.

In addition, we assessed homogeneity by comparing relative abundance values between aliquots of a given cohort. In the future, we plan to include the use of exogenous strain(s) whole cells added to the stool material during production to serve as an internal control. By adding an exogenous strain at equal cellular counts, we have an internal standard for comparing relative abundance between cohorts and an additional measurement of homogeneity. Regardless of whether we are using native taxa or internal standards, agreement will need to be reached on an acceptable CV between aliquots.

There are a few other measurands to consider related to metagenomic measurements including: DNA concentration, total bacterial abundance (using 16s digital polymerase chain reaction) and targeting fungal and viral members of the community. These methods would provide additional useful information not captured in the current workflow.

NMR, LC-MS, and GC-MS techniques all revealed metabolite differences between diets. The preservation method introduced some metabolite inconsistencies between materials, but diet had a greater contribution to the variance observed in multivariate analyses. Therefore, we proposed to move forward with two different aqueous fecal materials to represent the range in metabolites that may be observed with varying diets. In addition, aqueous preservation is more representative of a fresh stool sample than the lyophilized preservation.

The initial characterization via ^1H NMR showed that omnivore samples presented more data variability than vegan samples, which we speculate is from the hydrophobic layer formed during centrifugation. Across all samples, the aqueous extraction protocol extracted several SCFAs and amino acids expected to be found in a health individual. Some of the identified metabolites were present only in one material and in a few cases only in one vial replicate.

These are results that should be investigated closer by adding other NMR approaches and spike-in of known metabolites.

Vegan and omnivore samples had distinct metabolites according to the LC-MS based metabolomics but not between preservation methods. Regarding metabolite annotation, the most abundant metabolites may not be representative of the most concentrated metabolites in the samples due to ion suppression that may occur during electrospray ionization. Regardless, the technique provides a fingerprint of metabolites found in these two diets that can be used in further characterization.

On the other hand, qualitative analysis of SCFAs revealed differences between preservation methods via GC-MS with more abundant metabolites in lyophilized samples. Although an unexpected result, it may have occurred due the greater availability of the metabolites in the lyophilized samples as opposed the aqueous samples. Physicochemical characteristics of the aqueous samples such as hydrogen bonding may have delayed the desorption of the metabolites. However, for a such complex material, this is only a theory and should be evaluated in further analysis.

Differences in diet were revealed by the elevated levels of terpenes in vegan aqueous samples as opposed to omnivore aqueous samples. On the hand, relative abundance of terpenes was greater in aqueous samples suggesting that lyophilization may lead to losses of these compounds. In addition, competitive sorption between SCFAs and terpenes to the SPME fiber may have biased the detection of terpenes in lyophilized samples. Static headspace extraction could be used in future analysis to understand some of these biases.

It should be stated that these samples are not an authentic representation of human stool as they were pre-processed (homogenized and diluted in water or lyophilized) after collection for research application. Also, it should be highlighted that this report reflects the initial characterization for a research grade test material (RGTM) in the fall of 2020, which was distributed to the community to acquire feedback and determine its fit for purpose for future RM production. Since then, the manufacturer of the material has changed and the protocols described here to produce and analyze the materials have been further optimized. Lessons learned in the initial characterization described in this report will be applied to the actual reference material (RM 8048), including production of the material in a single batch, cryogenic homogenization, and blending with water for ease of sample handling. Homogeneity and stability measurements for RM 8048 will be included for all characterization endpoints 1) metagenomics to measure microbial composition, 2) LC-MS and NMR spectroscopy to qualitatively analyze the material by producing a list of annotated metabolites, and 3) flow cytometry to assess changes in microbial composition over time.

8. References

1. Ten Hoopen, P., et al., *The metagenomic data life-cycle: standards and best practices*. Gigascience, 2017. **6**(8): p. 1-11.
2. Amos, G.C.A., et al., *Developing standards for the microbiome field*. Microbiome, 2020. **8**(1): p. 98.
3. Sumner, L.W., et al., *Proposed minimum reporting standards for chemical analysis Chemical Analysis Working Group (CAWG) Metabolomics Standards Initiative (MSI)*. Metabolomics, 2007. **3**(3): p. 211-221.
4. Wilson, I.D., G. Theodoridis, and C. Virgiliou, *A perspective on the standards describing mass spectrometry-based metabolic phenotyping (metabolomics/metabonomics) studies in publications*. J Chromatogr B Analyt Technol Biomed Life Sci, 2021. **1164**: p. 122515.
5. Clemente, J.C., et al., *The impact of the gut microbiota on human health: an integrative view*. Cell, 2012. **148**(6): p. 1258-70.
6. Valdes, A.M., et al., *Role of the gut microbiota in nutrition and health*. BMJ, 2018. **361**: p. k2179.
7. Zimmermann, M., et al., *Mapping human microbiome drug metabolism by gut bacteria and their genes*. Nature, 2019. **570**(7762): p. 462-467.
8. Mandal, R., et al., *Workshop report: Toward the development of a human whole stool reference material for metabolomic and metagenomic gut microbiome measurements*. Metabolomics, 2020. **16**(11): p. 119.
9. Karu, N., et al., *A review on human fecal metabolomics: Methods, applications and the human fecal metabolome database*. Anal Chim Acta, 2018. **1030**: p. 1-24.
10. Bojanova, D.P. and S.R. Bordenstein, *Fecal Transplants: What Is Being Transferred?* PLoS Biol, 2016. **14**(7): p. e1002503.
11. Cabrol, L., M. Quemeneur, and B. Misson, *Inhibitory effects of sodium azide on microbial growth in experimental resuspension of marine sediment*. J Microbiol Methods, 2017. **133**: p. 62-65.

Appendix A. Genera and Relative Abundance for 10 replicate Vegan aliquots.

Taxonomy ID	Genus	139342_ Vegan1	139369_ Vegan2	139407_ Vegan3	139440_ Vegan4	139445_ Vegan5	139585_ Vegan6	139623_ Vegan7	139696_ Vegan8	139804_ Vegan9	139851_ Vegan10
1263	Ruminococcus	0.1620	0.1565	0.1653	0.1699	0.1504	0.1632	0.1725	0.1731	0.1696	0.1634
1678	Bifidobacterium	0.1115	0.1161	0.1079	0.1252	0.1103	0.1000	0.1080	0.1256	0.1263	0.1071
572511	Blautia	0.0841	0.0847	0.0867	0.0814	0.0883	0.0914	0.0999	0.0936	0.0930	0.0949
186803	Lachnospiraceae_u_g	0.0722	0.0753	0.0794	0.0735	0.0724	0.0827	0.0874	0.0928	0.0872	0.0867
816	Bacteroides	0.0936	0.0946	0.0925	0.0863	0.0980	0.0851	0.0631	0.0416	0.0553	0.0652
33042	Coprococcus	0.0633	0.0656	0.0675	0.0599	0.0608	0.0755	0.0766	0.0822	0.0728	0.0731
189330	Dorea	0.0405	0.0407	0.0423	0.0410	0.0401	0.0442	0.0484	0.0495	0.0470	0.0476
239759	Alistipes	0.0620	0.0577	0.0469	0.0527	0.0720	0.0351	0.0313	0.0180	0.0261	0.0328
102106	Collinsella	0.0337	0.0324	0.0338	0.0334	0.0300	0.0332	0.0383	0.0346	0.0338	0.0364
1730	Eubacterium	0.0268	0.0283	0.0287	0.0283	0.0276	0.0318	0.0320	0.0352	0.0345	0.0329
39948	Dialister	0.0334	0.0309	0.0275	0.0321	0.0292	0.0263	0.0186	0.0251	0.0298	0.0319
207244	Anaerostipes	0.0234	0.0258	0.0265	0.0238	0.0252	0.0295	0.0345	0.0362	0.0296	0.0302
1485	Clostridium	0.0182	0.0187	0.0200	0.0197	0.0192	0.0223	0.0226	0.0303	0.0259	0.0245
239934	Akkermansia	0.0196	0.0183	0.0192	0.0200	0.0233	0.0203	0.0222	0.0171	0.0174	0.0203
841	Roseburia	0.0186	0.0206	0.0194	0.0194	0.0199	0.0207	0.0192	0.0185	0.0200	0.0204
216851	Faecalibacterium	0.0169	0.0170	0.0170	0.0157	0.0186	0.0183	0.0178	0.0168	0.0150	0.0161
2172	Methanobrevibacter	0.0125	0.0137	0.0140	0.0132	0.0121	0.0166	0.0192	0.0218	0.0173	0.0163
2	Bacteria_u_g	0.0069	0.0068	0.0093	0.0093	0.0059	0.0112	0.0122	0.0136	0.0106	0.0121
375288	Parabacteroides	0.0117	0.0109	0.0122	0.0095	0.0116	0.0093	0.0078	0.0043	0.0073	0.0084
644652	Gordonibacter	0.0073	0.0061	0.0061	0.0069	0.0065	0.0061	0.0070	0.0051	0.0062	0.0076
1508657	Ruminiclostridium	0.0067	0.0076	0.0067	0.0069	0.0061	0.0064	0.0057	0.0055	0.0061	0.0061
838	Prevotella	0.0058	0.0052	0.0054	0.0052	0.0062	0.0056	0.0051	0.0030	0.0041	0.0051
186802	Clostridiales_u_g	0.0049	0.0042	0.0048	0.0043	0.0043	0.0065	0.0041	0.0048	0.0052	0.0049
447020	Adlercreutzia	0.0050	0.0048	0.0047	0.0053	0.0053	0.0039	0.0045	0.0038	0.0046	0.0050

NIST IR 8451
September 2023

459786	Oscillibacter	0.0050	0.0048	0.0044	0.0045	0.0053	0.0043	0.0038	0.0036	0.0037	0.0037
1573535	Holdemanela	0.0034	0.0036	0.0042	0.0040	0.0037	0.0043	0.0047	0.0043	0.0046	0.0047
292632	Subdoligranulum	0.0042	0.0043	0.0042	0.0044	0.0038	0.0039	0.0039	0.0032	0.0036	0.0040
135858	Catenibacterium	0.0028	0.0027	0.0035	0.0029	0.0024	0.0042	0.0040	0.0038	0.0042	0.0038
397864	Barnesiella	0.0049	0.0044	0.0036	0.0041	0.0052	0.0023	0.0019	0.0013	0.0017	0.0021
1301	Streptococcus	0.0026	0.0027	0.0029	0.0027	0.0026	0.0031	0.0018	0.0045	0.0031	0.0025
990721	Christensenella	0.0029	0.0028	0.0027	0.0031	0.0027	0.0027	0.0029	0.0028	0.0029	0.0029
84111	Eggerthella	0.0030	0.0028	0.0029	0.0032	0.0026	0.0026	0.0014	0.0022	0.0028	0.0033
33024	Phascolarctobacterium	0.0026	0.0026	0.0028	0.0027	0.0025	0.0025	0.0026	0.0018	0.0022	0.0028
1573534	Faecalitalea	0.0021	0.0022	0.0022	0.0023	0.0022	0.0022	0.0025	0.0025	0.0025	0.0026
1473205	Senegalimassilia	0.0019	0.0018	0.0018	0.0020	0.0020	0.0019	0.0020	0.0017	0.0021	0.0023
872	Desulfovibrio	0.0021	0.0019	0.0016	0.0015	0.0022	0.0023	0.0022	0.0011	0.0016	0.0020
171549	Bacteroidales_u_g	0.0022	0.0030	0.0022	0.0000	0.0046	0.0016	0.0000	0.0017	0.0010	0.0000
1350	Enterococcus	0.0022	0.0022	0.0020	0.0024	0.0003	0.0011	0.0006	0.0020	0.0010	0.0023
61170	Holdemania	0.0015	0.0014	0.0015	0.0018	0.0016	0.0013	0.0014	0.0011	0.0015	0.0014
1506553	Lachnoclostridium	0.0010	0.0010	0.0009	0.0018	0.0012	0.0011	0.0007	0.0006	0.0010	0.0011
1654	Actinomyces	0.0007	0.0007	0.0009	0.0011	0.0012	0.0011	0.0007	0.0011	0.0014	0.0009
1506577	Tyzzerella	0.0008	0.0009	0.0009	0.0008	0.0009	0.0009	0.0009	0.0009	0.0009	0.0009
128827	Erysipelotrichaceae_u_g	0.0012	0.0009	0.0003	0.0015	0.0003	0.0003	0.0000	0.0011	0.0020	0.0010
846	Oxalobacter	0.0008	0.0007	0.0011	0.0008	0.0012	0.0004	0.0010	0.0004	0.0006	0.0007
216572	Oscillospiraceae_u_g	0.0009	0.0008	0.0007	0.0006	0.0009	0.0009	0.0006	0.0005	0.0006	0.0006
186804	Peptostreptococcaceae_u_g	0.0012	0.0011	0.0013	0.0000	0.0000	0.0009	0.0000	0.0011	0.0009	0.0000
32207	Rothia	0.0004	0.0004	0.0004	0.0005	0.0005	0.0005	0.0005	0.0006	0.0008	0.0004
35832	Bilophila	0.0012	0.0007	0.0003	0.0002	0.0004	0.0008	0.0000	0.0003	0.0006	0.0004
31979	Clostridiaceae_u_g	0.0004	0.0005	0.0005	0.0005	0.0004	0.0004	0.0000	0.0000	0.0012	0.0005
577309	Paraprevotella	0.0004	0.0004	0.0003	0.0004	0.0005	0.0007	0.0000	0.0004	0.0005	0.0002
1392389	Intestinimonas	0.0005	0.0005	0.0005	0.0005	0.0006	0.0005	0.0000	0.0000	0.0002	0.0004
283168	Odoribacter	0.0006	0.0006	0.0006	0.0006	0.0007	0.0003	0.0000	0.0000	0.0000	0.0002
830	Butyrivibrio	0.0003	0.0003	0.0004	0.0004	0.0003	0.0004	0.0004	0.0004	0.0004	0.0004

NIST IR 8451
September 2023

1243	Leuconostoc	0.0003	0.0003	0.0003	0.0002	0.0002	0.0003	0.0003	0.0006	0.0006	0.0004
1505663	Erysipelatoclostridium	0.0002	0.0003	0.0000	0.0006	0.0002	0.0005	0.0000	0.0003	0.0004	0.0006
80840	Burkholderiales_u_g	0.0000	0.0008	0.0008	0.0000	0.0000	0.0007	0.0000	0.0003	0.0005	0.0000
946234	Flavonifractor	0.0002	0.0004	0.0004	0.0002	0.0002	0.0004	0.0004	0.0003	0.0003	0.0002
1357	Lactococcus	0.0002	0.0003	0.0003	0.0003	0.0003	0.0003	0.0005	0.0003	0.0003	0.0003
649777	Synergistaceae_u_g	0.0006	0.0004	0.0005	0.0000	0.0000	0.0005	0.0000	0.0003	0.0004	0.0000
1578	Lactobacillus	0.0005	0.0000	0.0005	0.0003	0.0000	0.0002	0.0003	0.0003	0.0005	0.0000
244127	Anaerotruncus	0.0003	0.0003	0.0003	0.0003	0.0003	0.0003	0.0000	0.0000	0.0003	0.0003
1649459	Hungatella	0.0003	0.0002	0.0002	0.0002	0.0002	0.0003	0.0003	0.0003	0.0002	0.0002
541000	Ruminococcaceae_u_g	0.0003	0.0003	0.0003	0.0003	0.0003	0.0003	0.0000	0.0000	0.0003	0.0003
574697	Butyricimonas	0.0003	0.0003	0.0004	0.0003	0.0004	0.0004	0.0000	0.0000	0.0002	0.0000
264995	Anaerofustis	0.0002	0.0002	0.0003	0.0003	0.0000	0.0003	0.0000	0.0000	0.0003	0.0003
1870884	Clostridioides	0.0000	0.0000	0.0000	0.0016	0.0000	0.0000	0.0000	0.0000	0.0000	0.0000
1017280	Pseudoflavonifractor	0.0002	0.0002	0.0000	0.0002	0.0002	0.0002	0.0000	0.0000	0.0002	0.0002
40544	Sutterella	0.0012	0.0000	0.0000	0.0000	0.0002	0.0000	0.0000	0.0000	0.0000	0.0000
577310	Parasutterella	0.0004	0.0000	0.0000	0.0004	0.0005	0.0000	0.0000	0.0000	0.0000	0.0000
1505657	Intestinibacter	0.0000	0.0000	0.0000	0.0002	0.0003	0.0000	0.0000	0.0004	0.0003	0.0000
904	Acidaminococcus	0.0000	0.0000	0.0000	0.0000	0.0000	0.0006	0.0000	0.0000	0.0005	0.0000
580024	Enterorhabdus	0.0003	0.0003	0.0002	0.0000	0.0000	0.0000	0.0000	0.0000	0.0003	0.0000
184869	Varibaculum	0.0000	0.0003	0.0003	0.0003	0.0000	0.0000	0.0000	0.0000	0.0000	0.0000
1164882	Lachnoanaerobaculum	0.0000	0.0000	0.0000	0.0000	0.0000	0.0003	0.0000	0.0000	0.0002	0.0002
724	Haemophilus	0.0000	0.0002	0.0000	0.0002	0.0002	0.0000	0.0000	0.0000	0.0000	0.0000
2048137	Agathobaculum	0.0002	0.0000	0.0000	0.0002	0.0002	0.0000	0.0000	0.0000	0.0000	0.0000
1165076	Imtechella	0.0000	0.0000	0.0003	0.0000	0.0002	0.0000	0.0000	0.0000	0.0000	0.0000
1386	Bacillus	0.0002	0.0000	0.0000	0.0000	0.0000	0.0000	0.0000	0.0000	0.0002	0.0000
906	Megasphaera	0.0002	0.0000	0.0000	0.0000	0.0000	0.0000	0.0000	0.0000	0.0000	0.0000

Appendix B. Genera and Relative Abundance for 10 replicate Omnivore aliquots

Taxonomy Id	Genus	138274_ Omni1	138348_ Omni2	138390_ Omni3	138436_ Omni4	138483_ Omni5	138505_ Omni6	138551_ Omni7	138588_ Omni8	138714_ Omni9	138756_ Omni10
816	Bacteroides	0.1475	0.1466	0.1608	0.1662	0.1454	0.1622	0.1260	0.1104	0.1169	0.1319
572511	Blautia	0.1179	0.1205	0.1161	0.1130	0.1084	0.1422	0.1278	0.1330	0.1259	0.1245
1263	Ruminococcus	0.0855	0.0879	0.0902	0.0837	0.0834	0.1107	0.0961	0.0986	0.0943	0.0957
186803	Lachnospiraceae_u_g	0.0816	0.0884	0.0762	0.0795	0.0813	0.1226	0.0970	0.1000	0.0977	0.0980
1678	Bifidobacterium	0.1069	0.0897	0.0888	0.0988	0.1007	0.0323	0.0856	0.0913	0.0908	0.0866
33042	Coprococcus	0.0450	0.0457	0.0466	0.0441	0.0424	0.0560	0.0486	0.0535	0.0482	0.0482
239759	Alistipes	0.0603	0.0575	0.0706	0.0580	0.0668	0.0187	0.0369	0.0310	0.0370	0.0378
102106	Collinsella	0.0431	0.0431	0.0377	0.0441	0.0477	0.0163	0.0425	0.0449	0.0444	0.0417
189330	Dorea	0.0320	0.0341	0.0299	0.0306	0.0298	0.0405	0.0350	0.0349	0.0337	0.0339
1730	Eubacterium	0.0276	0.0296	0.0270	0.0265	0.0268	0.0465	0.0337	0.0331	0.0328	0.0339
216851	Faecalibacterium	0.0296	0.0289	0.0335	0.0303	0.0318	0.0185	0.0329	0.0366	0.0358	0.0343
207244	Anaerostipes	0.0176	0.0181	0.0165	0.0159	0.0148	0.0264	0.0195	0.0214	0.0194	0.0205
128827	Erysipelotrichaceae_u_g	0.0161	0.0169	0.0150	0.0175	0.0184	0.0212	0.0181	0.0176	0.0187	0.0169
841	Roseburia	0.0168	0.0163	0.0169	0.0150	0.0168	0.0148	0.0173	0.0170	0.0172	0.0169
84111	Eggerthella	0.0171	0.0168	0.0160	0.0184	0.0219	0.0028	0.0165	0.0162	0.0174	0.0157
1485	Clostridium	0.0111	0.0129	0.0114	0.0107	0.0110	0.0204	0.0143	0.0134	0.0136	0.0144
186802	Clostridiales_u_g	0.0118	0.0127	0.0129	0.0125	0.0122	0.0137	0.0139	0.0130	0.0142	0.0135
375288	Parabacteroides	0.0117	0.0165	0.0117	0.0154	0.0099	0.0160	0.0105	0.0108	0.0158	0.0098
1573535	Holdemanella	0.0089	0.0102	0.0074	0.0088	0.0078	0.0181	0.0121	0.0116	0.0113	0.0119
459786	Oscillibacter	0.0097	0.0091	0.0116	0.0108	0.0116	0.0042	0.0103	0.0101	0.0103	0.0098
1506577	Tyzzarella	0.0071	0.0074	0.0102	0.0071	0.0076	0.0117	0.0094	0.0093	0.0095	0.0099
33024	Phascolarctobacterium	0.0087	0.0089	0.0084	0.0092	0.0095	0.0096	0.0090	0.0084	0.0083	0.0084
1870884	Clostridioides	0.0087	0.0086	0.0081	0.0094	0.0107	0.0014	0.0086	0.0082	0.0087	0.0080
1506553	Lachnoclostridium	0.0067	0.0066	0.0084	0.0070	0.0089	0.0059	0.0073	0.0071	0.0070	0.0069
1508657	Ruminiclostridium	0.0077	0.0076	0.0061	0.0064	0.0069	0.0062	0.0068	0.0063	0.0071	0.0070
2	Bacteria_u_g	0.0037	0.0047	0.0029	0.0038	0.0034	0.0136	0.0064	0.0053	0.0059	0.0065

NIST IR 8451
September 2023

1301	Streptococcus	0.0041	0.0044	0.0061	0.0039	0.0050	0.0076	0.0056	0.0063	0.0063	0.0065
39948	Dialister	0.0050	0.0053	0.0054	0.0059	0.0063	0.0037	0.0055	0.0056	0.0055	0.0050
447020	Adlercreutzia	0.0048	0.0046	0.0046	0.0058	0.0066	0.0008	0.0044	0.0043	0.0048	0.0042
1350	Enterococcus	0.0044	0.0019	0.0033	0.0029	0.0042	0.0051	0.0053	0.0048	0.0032	0.0046
1505663	Erysipelatoclostridium	0.0035	0.0035	0.0030	0.0017	0.0040	0.0069	0.0038	0.0035	0.0048	0.0035
836	Porphyromonas	0.0034	0.0026	0.0022	0.0030	0.0021	0.0029	0.0023	0.0043	0.0025	0.0026
239934	Akkermansia	0.0025	0.0024	0.0024	0.0028	0.0028	0.0011	0.0028	0.0026	0.0026	0.0025
644652	Gordonibacter	0.0026	0.0027	0.0023	0.0027	0.0035	0.0003	0.0026	0.0024	0.0028	0.0025
35832	Bilophila	0.0024	0.0022	0.0018	0.0025	0.0018	0.0008	0.0026	0.0027	0.0023	0.0024
397864	Barnesiella	0.0029	0.0029	0.0032	0.0025	0.0027	0.0017	0.0014	0.0010	0.0013	0.0013
946234	Flavonifractor	0.0020	0.0020	0.0022	0.0020	0.0021	0.0008	0.0022	0.0021	0.0022	0.0022
216572	Oscillospiraceae_u_g	0.0020	0.0017	0.0026	0.0017	0.0023	0.0009	0.0021	0.0022	0.0022	0.0021
577309	Paraprevotella	0.0019	0.0020	0.0023	0.0020	0.0022	0.0014	0.0018	0.0013	0.0016	0.0016
990721	Christensenella	0.0016	0.0015	0.0016	0.0016	0.0018	0.0017	0.0017	0.0018	0.0017	0.0017
292632	Subdoligranulum	0.0017	0.0017	0.0018	0.0019	0.0022	0.0008	0.0016	0.0016	0.0016	0.0016
80840	Burkholderiales_u_g	0.0012	0.0012	0.0016	0.0017	0.0010	0.0009	0.0012	0.0011	0.0013	0.0012
577310	Parasutterella	0.0015	0.0012	0.0017	0.0014	0.0011	0.0009	0.0013	0.0010	0.0011	0.0011
1743	Propionibacterium	0.0010	0.0009	0.0014	0.0012	0.0016	0.0004	0.0012	0.0011	0.0015	0.0012
100883	Coprobacillus	0.0000	0.0002	0.0007	0.0008	0.0007	0.0028	0.0012	0.0011	0.0012	0.0012
244127	Anaerotruncus	0.0009	0.0009	0.0009	0.0009	0.0011	0.0007	0.0010	0.0009	0.0009	0.0009
186804	Peptostreptococcaceae_u_g	0.0009	0.0007	0.0011	0.0009	0.0012	0.0008	0.0005	0.0008	0.0006	0.0005
171549	Bacteroidales_u_g	0.0025	0.0008	0.0010	0.0002	0.0006	0.0000	0.0002	0.0000	0.0002	0.0013
830	Butyrivibrio	0.0005	0.0006	0.0005	0.0005	0.0005	0.0007	0.0006	0.0006	0.0006	0.0006
561	Escherichia	0.0014	0.0013	0.0000	0.0004	0.0003	0.0003	0.0008	0.0000	0.0007	0.0003
283168	Odoribacter	0.0007	0.0007	0.0009	0.0007	0.0008	0.0003	0.0003	0.0000	0.0002	0.0003
40544	Sutterella	0.0010	0.0011	0.0003	0.0022	0.0002	0.0000	0.0000	0.0000	0.0000	0.0000
1649459	Hungatella	0.0004	0.0004	0.0005	0.0004	0.0005	0.0004	0.0004	0.0005	0.0004	0.0004
1392389	Intestinimonas	0.0005	0.0005	0.0006	0.0005	0.0005	0.0000	0.0004	0.0002	0.0004	0.0004
1472649	Dielma	0.0004	0.0004	0.0003	0.0003	0.0004	0.0006	0.0004	0.0003	0.0005	0.0004

NIST IR 8451
September 2023

580024	Enterorhabdus	0.0005	0.0004	0.0004	0.0005	0.0006	0.0000	0.0004	0.0004	0.0004	0.0004
2057233	Absiella	0.0003	0.0004	0.0003	0.0003	0.0003	0.0006	0.0004	0.0004	0.0004	0.0005
1357	Lactococcus	0.0004	0.0002	0.0002	0.0004	0.0003	0.0004	0.0003	0.0004	0.0003	0.0003
574697	Butyricimonas	0.0006	0.0006	0.0002	0.0003	0.0002	0.0003	0.0000	0.0000	0.0002	0.0002
541000	Ruminococcaceae_u_g	0.0002	0.0002	0.0003	0.0003	0.0003	0.0000	0.0002	0.0003	0.0002	0.0003
649777	Synergistaceae_u_g	0.0003	0.0002	0.0003	0.0003	0.0000	0.0000	0.0003	0.0002	0.0003	0.0003
32207	Rothia	0.0000	0.0002	0.0003	0.0002	0.0003	0.0000	0.0000	0.0010	0.0000	0.0000
1578	Lactobacillus	0.0000	0.0002	0.0000	0.0000	0.0002	0.0000	0.0005	0.0002	0.0005	0.0002
61170	Holdemania	0.0002	0.0002	0.0002	0.0002	0.0003	0.0000	0.0002	0.0000	0.0002	0.0002
1505657	Intestinibacter	0.0000	0.0000	0.0000	0.0000	0.0000	0.0007	0.0003	0.0000	0.0003	0.0003
1654	Actinomyces	0.0000	0.0000	0.0003	0.0000	0.0002	0.0000	0.0000	0.0000	0.0003	0.0000
1573534	Faecalitalea	0.0000	0.0000	0.0000	0.0000	0.0005	0.0000	0.0000	0.0000	0.0000	0.0000
28050	Lachnospira	0.0000	0.0000	0.0000	0.0000	0.0001	0.0003	0.0000	0.0000	0.0000	0.0000
29465	Veillonella	0.0000	0.0000	0.0000	0.0000	0.0002	0.0000	0.0000	0.0000	0.0000	0.0002
1017280	Pseudoflavonifractor	0.0000	0.0000	0.0002	0.0000	0.0002	0.0000	0.0000	0.0000	0.0000	0.0000
904	Acidaminococcus	0.0000	0.0000	0.0000	0.0000	0.0000	0.0000	0.0000	0.0000	0.0000	0.0002
2753	Synergistes	0.0000	0.0000	0.0000	0.0000	0.0002	0.0000	0.0000	0.0000	0.0000	0.0000
838	Prevotella	0.0000	0.0000	0.0000	0.0000	0.0000	0.0000	0.0002	0.0000	0.0000	0.0000
724	Haemophilus	0.0000	0.0000	0.0000	0.0000	0.0000	0.0002	0.0000	0.0000	0.0000	0.0000
1165076	Imtechella	0.0000	0.0000	0.0000	0.0000	0.0000	0.0000	0.0002	0.0000	0.0000	0.0000
846	Oxalobacter	0.0000	0.0000	0.0000	0.0000	0.0002	0.0000	0.0000	0.0000	0.0000	0.0000
248744	Marvinbryantia	0.0000	0.0000	0.0000	0.0000	0.0001	0.0000	0.0000	0.0000	0.0000	0.0000

Appendix C. Metabolite concentration (mM) in the NMR sample extract relative to the TMS chemical shift reference standard. Four vials were analyzed per each sample.

	Vegan-Aq				Vegan-Ly				Omni-Aq				Omni-Ly			
	Mean	SD	relSD%	N ¹	Mean	SD	relSD%	N ¹	Mean	SD	relSD%	N ¹	Mean	SD	relSD%	N ¹
1,3-Dihydroxyacetone	0.013	0.001	7.0	4	0.002	0.000	8.2	3	0.013	0.010	75.4	4	0.009	0.002	22.2	4
2-Methylglutarate				0	0.042	0.065	153.8	4				0	0.065	0.061	94.8	3
3-Hydroxybutyrate	0.005			1	0.009			1				0				0
3-Hydroxyphenylacetate	0.015	0.002	13.9	4	0.008	0.000	5.0	4	0.008	0.001	14.8	4	0.009	0.003	38.7	4
3-Methyl-2-oxovalerate	0.015	0.001	9.6	4	0.015	0.002	15.4	4	0.023	0.012	51.7	2	0.009	0.004	43.1	4
4-Pyridoxate	0.003	0.000	8.3	4	0.003	0.001	31.2	4	0.003	0.001	43.7	4	0.003	0.001	25.3	4
Acetate	4.419	0.204	12.2	4	3.289	0.368	11.2	4	3.831	0.806	21.0	4	1.784	0.684	38.3	4
Alanine	0.248	0.024	9.8	4	0.013	0.008	61.7	2	0.354	0.189	53.3	4				0
Butyrate	1.017	0.116	11.4	4	0.663	0.064	9.7	4	0.863	0.294	34.0	4	0.526	0.258	49.1	4
Caprate	0.075	0.006	8.5	4	0.147	0.016	10.6	4	0.109	0.035	32.3	4	0.106	0.033	30.6	4
Choline	0.005	0.000	3.6	4	0.008	0.001	17.9	4	0.004	0.002	41.6	4	0.003	0.002	51.8	4
Ethanol				0				0	0.190	0.038	20.2	4				0
Formate	0.011	0.002	16.9	4	0.011	0.002	17.3	4	0.024	0.031	130.4	4	0.007	0.004	47.1	4
Fumarate	0.043	0.005	11.4	4	0.020	0.002	11.1	4	0.048	0.031	65.9	4	0.021	0.007	31.8	4
Galactose	0.110	0.021	19.4	4	0.138	0.054	38.9	4	0.114	0.038	33.6	4	0.107	0.013	12.6	4
Glucose	0.274	0.045	16.5	4	0.328	0.035	10.8	4	0.331	0.153	46.2	4	0.212	0.073	34.5	4
Glutamate	0.421	0.057	13.6	4	0.510	0.062	12.1	4	0.603	0.295	48.9	4	0.446	0.229	51.4	4
Glutamine	0.137	0.017	12.1	4	0.155	0.052	33.8	4	0.157	0.041	26.5	4	0.114	0.041	35.7	4
Glutarate				0				0				0	0.063	0.015	23.3	3
Glycerol	0.313	0.007	2.2	4	0.407	0.042	10.4	4	0.294	0.021	7.3	3	0.295	0.115	39.0	4
Glycine	0.010	0.001	6.7	4	0.008	0.001	9.3	4	0.031	0.045	148.3	4	0.008	0.005	55.2	4
Homovanillate	0.005	0.001	17.3	4	0.004	0.001	17.9	4	0.004	0.000	8.2	4	0.005	0.002	38.4	4
Isobutyrate	0.139	0.019	13.7	4				0	0.134	0.031	23.1	4	0.037	0.022	59.7	3

Isoleucine	0.065	0.007	11.3	4	0.115	0.059	51.0	4	0.081	0.017	20.4	4	0.080	0.067	83.0	4
Isovalerate	0.112	0.013	11.5	4	0.124	0.020	16.2	4	0.098	0.022	22.2	4	0.072	0.022	30.4	4
Lactate	0.026	0.002	7.8	3	0.048	0.010	21.2	4	0.027			1	0.023	0.002	7.0	3
Leucine	0.111	0.005	4.5	4	0.174	0.024	14.0	4	0.155	0.076	48.9	4	0.149	0.059	39.3	4
Malonate	0.019	0.001	3.7	4	0.054	0.007	12.1	4	0.102	0.024	23.3	4	0.094	0.033	35.0	4
Mannitol	0.084	0.006	6.8	4	0.029			1	0.079	0.012	15.2	4	0.044			1
Mannose	0.020	0.005	25.4	3	0.020	0.003	13.5	3				0	0.157	0.139	88.5	3
Methionine	0.055	0.004	7.4	4	0.073	0.009	11.8	4	0.084	0.029	34.5	4	0.059	0.033	55.6	4
Proline	0.114	0.019	16.7	4	0.126	0.049	38.8	2	0.144	0.081	56.2	4				0
Propionate	0.918	0.102	11.2	4	0.492	0.233	47.5	2	1.146	0.256	22.3	4	0.558	0.281	50.3	4
Pyruvate	0.015	0.004	28.9	4	0.009	0.001	5.3	4	0.013	0.001	4.7	4	0.006	0.003	42.0	4
Succinate	0.011	0.002	15.7	4	0.011	0.003	24.3	4	0.035	0.010	30.0	4	0.022	0.008	37.3	4
Taurine				0	0.020	0.006	31.1	3	0.055	0.008	14.3	2	0.033	0.004	13.0	2
Theophylline	0.001	0.000	33.0	3	0.001	0.000	36.3	4	0.001	0.000	17.5	4	0.001	0.000	6.7	2
Threonine	0.113	0.004	4.0	4	0.132	0.011	8.1	4	0.163	0.090	55.4	4	0.128	0.068	53.0	4
Tryptophan	0.013	0.002	15.1	3	0.017	0.003	18.2	4	0.018	0.003	15.1	4	0.017	0.004	23.9	4
Uracil	0.049	0.003	5.4	4	0.058	0.006	11.0	4	0.042	0.003	7.7	3	0.036	0.003	9.0	3
Valerate	0.166	0.019	11.5	4	0.563	0.075	13.3	4	0.260	0.069	26.5	4	0.193	0.077	40.1	4
Valine	0.167	0.012	7.1	4	0.135	0.020	14.7	4	0.226	0.128	56.7	4	0.123	0.042	34.4	4
Xanthine	0.059	0.003	5.1	3	0.067	0.004	5.5	4	0.052	0.003	5.4	2	0.045	0.003	7.6	3
Xylose	0.088	0.026	29.0	4	0.098	0.009	9.5	4	0.088	0.036	41.2	4	0.098	0.036	37.2	4
p-Cresol	0.020	0.003	13.2	4	0.024	0.003	13.4	4	0.019	0.003	16.0	4	0.020	0.006	30.3	4

¹Metabolites observed in *n* number of vials

Appendix D. Glossary

%RSD	Relative standard deviation in percentage
¹ H NMR	Proton nuclear magnetic resonance spectroscopy
CH ₃ OD	Deuterated methanol
CPMG	Carr-Purcell-Meiboom-Gill
D ₂ O	Deuterium oxide
GCxGC-TOFMS-MS	Two-dimensional gas chromatography coupled to a time-of-flight mass spectrometer
HCD	Higher-energy C-trap dissociation
HSS	High Strength Silica
IRB	Institutional review board
LC-HRMS	Liquid chromatography high resolution mass spectrometry
MeOH	Methanol
MTA	Material transfer agreement
NIST	National Institute of Standards and Technology
NOESY	Nuclear Overhauser Effect Spectroscopy
Omni-Aq, OA	Omnivore aqueous
Omni-Ly, OL	Omnivore lyophilized
PCA	Principal component analysis
RGTM	Research grade testing material
RM	Reference material
SCFAs	Short chain fatty acids
SPME	Solid phase microextraction
TBC	The BioCollective
TMSP	Sodium-3-trimethylsilylpropionate
UPLC	Ultra-performance liquid chromatography
Vegan-Ly, VL	Vegan lyophilized
Vegan-Ly, VA	Vegan aqueous